

Article

The Climate-Growth Relationship between *Picea smithiana* (Wall.) Boiss. and *Abies pindrow* (Royle ex D. Don) Royle along the Latitudinal Gradient in Northern Pakistan

Habib Ullah ^{1,*} , Xiaochun Wang ^{1,*} , Quaid Hussain ^{2,*} , Abdullah Khan ³, Naveed Ahmad ⁴, Nizar Ali ⁵, Muhammad Waheed Riaz ²  and Izhar Hussain ⁶ 

- ¹ Key Laboratory of Sustainable Forest Ecosystem Management-Ministry of Education, School of Forestry, Northeast Forestry University, Harbin 150040, China
 - ² State Key Laboratory of Subtropical Silviculture, Zhejiang A&F University, 666 Wusu Street, Hangzhou 311300, China
 - ³ Department of Horticulture, Faculty of Agriculture Sciences, The University of Haripur, Haripur 22600, Pakistan
 - ⁴ Department of Forestry and Range Management, PMAS Arid Agriculture University, Rawalpindi 46300, Pakistan
 - ⁵ Department of Forestry and Wildlife Management, The University of Haripur, Haripur 22600, Pakistan
 - ⁶ Department of Plant Breeding and Genetics, The University of Haripur, Haripur 22600, Pakistan
- * Correspondence: wangx@nefu.edu.cn (X.W.); quaid_hussain@yahoo.com (Q.H.)



Citation: Ullah, H.; Wang, X.; Hussain, Q.; Khan, A.; Ahmad, N.; Ali, N.; Riaz, M.W.; Hussain, I. The Climate-Growth Relationship between *Picea smithiana* (Wall.) Boiss. and *Abies pindrow* (Royle ex D. Don) Royle along the Latitudinal Gradient in Northern Pakistan. *Forests* **2022**, *13*, 1315. <https://doi.org/10.3390/f13081315>

Academic Editor: John Innes

Received: 7 July 2022

Accepted: 15 August 2022

Published: 17 August 2022

Publisher's Note: MDPI stays neutral with regard to jurisdictional claims in published maps and institutional affiliations.



Copyright: © 2022 by the authors. Licensee MDPI, Basel, Switzerland. This article is an open access article distributed under the terms and conditions of the Creative Commons Attribution (CC BY) license (<https://creativecommons.org/licenses/by/4.0/>).

Abstract: A changing climate and global warming have adversely affected Pakistan's moist and dry temperate vegetation. *Abies pindrow* (fir) (Royle ex D. Don) Royle and *Picea smithiana* (spruce) Wall. Boiss are the two major representative species of the moist and dry temperate forests in Northern Pakistan. The dendroclimatic study of both species is crucial for the assessment of climate variability at various spatial and temporal scales. This study examined the dendroclimatology of fir and spruce, and analyzed the growth–climate relationship along the latitudinal gradient. Two hundred and nineteen samples (ring cores) of the two species were collected from five different sites (Shogran (SHG), Upper Dir (UDS), Bahrain Swat (BSG), Astore Gilgit (NPKA), and Sharan Kaghan (SHA)) in Northern Pakistan. The cores were cross-dated, and chronologies were generated for the species and climatic data (precipitation, temperature, and Palmer Drought Severity Index (PDSI)) correlated with radial growth. The interspecies correlations for fir were calculated as 0.54, 0.49, 0.52, 0.60, and 0.48 for SHG, UDS, BSG, NPKA, and SHA, respectively, whereas in the case of spruce, the interspecies correlations were 0.44 for SHG, 0.55 for UDS, and 0.49 for BSG. Climate variability was observed in the samples of both species, which showed significant drought and humid years at specific intervals. With respect to the correlation between tree-ring width and climatic factors, a positive correlation was observed between fir growth and summer season precipitation, mean temperature, and PDSI in the spring, summer, and autumn seasons. Similarly, the growth of spruce was positively correlated with precipitation (in February, September, and May) and PDSI (in the summer and autumn seasons); however, no correlation was observed between monthly temperature and spruce growth. The relationship of fir and spruce growth with seasonal precipitation and PDSI showed a change from a negative to a positive correlation after 1980, following rapid warming. During the winter and spring, the correlation coefficient between fir radial growth and seasonal temperature showed an initial upward trend followed by a progressive decrease along with increasing latitude. Seasonal variations were observed regarding the correlation coefficient between spruce radial growth and increasing latitude (increasing in winter; a decreasing trend in spring and summer; an initial increase and then a decrease in autumn). In the same way, the correlation of seasonal temperature and PDSI with the radial growth of both species showed increasing trends with increasing latitude, except in the autumn season.

Keywords: radial growth; *Picea smithiana*; *Abies pindrow*; dendroclimatology; climate change

1. Introduction

Climate change is a globally recognized environmental issue that seriously impacts natural resources, including forest ecosystems, floristic composition, and tree productivity [1]. Moreover, recent research by Stefanidis and Alexandridis [2] shows that the temporal changes in drought conditions also differ significantly between forest ecosystems of different types (broadleaved, coniferous) and climatic conditions. However, there are few studies covering the trend analysis of drought in forest ecosystems that are based on long-term time series from ground-based meteorological stations in mountain areas. This is because of the difficulties in installing and maintaining meteorological instruments, especially at high elevations in mountainous regions. Additionally, it is well-acknowledged that future climate projections will significantly affect forest growth and even result in the shifting of forest lines [3]. Over the most significant land region for which observational data are available for trend analysis, the frequency and severity of heavy precipitation events have increased since the 1950s, and human-induced climate change is likely the primary cause—this has been established with high confidence. Through increased land evapotranspiration, human-induced climate change has caused agricultural and ecological droughts in several locations—based on data with medium confidence [4]. There is low confidence in long-term trends in the frequency of all-category tropical cyclones (multi-decadal to centennial). Although data limitations prevent the accurate detection of historical trends on a global basis, event attribution studies and scientific understanding strongly suggest, with high confidence, that human-induced climate change increases the amount of heavy precipitation associated with tropical cyclones [4]. The accuracy of estimates of remaining carbon budgets has improved since the IPCC's Fifth Assessment Report (AR5), combined with new methods initially introduced in SR1.5, updated data, and the integration of findings from several lines of evidence. Consistent evaluation of the impacts of different assumptions on climate and air pollution projections requires the use of various potential future air pollution controls across scenarios. Finding the point at which climatic reactions to emissions reductions become detectable above the level of fluctuations due to internal variability and responses to natural factors is a significant development [4]. Over several decades, the changing climate has influenced vegetation structure, species combination, and growth dynamics [5,6]. Many tree species have been unable to adapt their physiology to escalating changes in climate [7]. The changing climate is mainly characterized by changes in two attributes, temperature and precipitation, which significantly affect vegetation ecology, its spatial distribution, health, and yield [8–10]. Such adverse climatic influences become more complicated in mountainous areas (specifically in moist and dry temperate forests) located in humid and subhumid ecological zones [11,12]. Tree radial growth data have been used worldwide to reconstruct the climatic variations occurring in the past hundreds of years at a regional level [13–18]. In this context, it is necessary to explore the growth response of forest trees to change over the last few decades, as such understanding helps researchers to quantify climatic influences over time [12,19].

Above-optimum warming enhances tree-ring width at higher altitudes [20,21], as reported in different parts of the world: in North America [22], in the mountains of Tianshan [23], in southeastern parts of Tibet [24], and in the Iranian Plateau [25]. Nonetheless, few studies are available regarding the growth–climatic relationship of different species along altitudinal gradients [12]. The responses of morphological attributes in trees are specific to the species, and the influence of a changing climate on growth may depend on wood density, tolerance to drought conditions, leaf morphology, and the volume of trees [26,27]. Temperatures that are higher than the optimum level may activate multiple responses in forest trees, including in phenology, decreased productivity, changes in altitudinal ranges, and the structure of plant communities [16,28,29]. Nevertheless, limited research is available on the growth sensitivity and anatomical responses of forest trees to changing climates [30,31]. The duration of the growing season and the prevalent temperature are two important factors that significantly influence growth–climate relationships [32,33]. Moreover, the

availability of moisture, nutrient deposition, and optimum precipitation greatly influence tree growth [31,34].

However, studies have found that relationships between climatic factors and corresponding tree growth are not always consistent [35]. Even individuals of the same species show variations in climate–growth relationships at different localities in the Himalayas [36,37]. Similarly, various tree species of the Himalayan forests show different growth responses to changing climates, as reported by [38]. One of the best examples demonstrating inconsistent growth–climate relationships is that of *Abies spectabilis* (D. Don) Spach 1841 [39], reported in several studies. Shrestha et al. [40] and Schwab et al. [21] reported a positive correlation between the temperature of the current and previous seasons and *Abies spectabilis* radial growth.

In contrast, Raybacket et al. [41] reported that temperature in the winter season is negatively correlated with radial growth. Similarly, Zhuang et al. [42] reported that a longer growing season and high temperature are positively correlated with radial growth. The extension of the growing season is directly linked with the temperature increase, which ultimately results in higher annual radial growth [43]. Moreover, Xu et al. [44] reported that water stress in the summer season might severely degrade the growth of coniferous trees because of higher evapotranspiration. Furthermore, a significant correlation between seasonal precipitation and tree radial growth has been noted, which varies according to different forest types [45].

In other studies, a strong correlation was reported between the width of spruce tree-rings and the past climate and summer temperatures, and moisture availability data were reconstructed from dendroclimatological analyses of spruce and fir [46–51]. A reconstruction based on conifer tree-rings indicated increasing drought stress and an upward trend for summer aridity with an immediate increase in warming over several decades [52]. Drought stress is positively correlated with spruce growth at lower altitudes, whereas coniferous trees at higher altitudes show an increased radial width with increases in temperature [53,54]. Therefore, the harshness of the climate along the altitudinal gradient strongly influences the response of tree growth to temperature and precipitation, although in different ways [55]: the former limits radial growth at higher altitudes [56–58], whereas the latter limits growth sensitivity at lower altitudes [59]. Similarly, various studies conducted along altitudinal and latitudinal gradients have reported that the winter temperature is positively correlated with radial growth [59–61]. In contrast, numerous studies have reported a negative correlation between the spring and early season temperature and radial growth at higher elevations [59] in the central part of the Himalayas [62,63], western Himalayas [64], and in southeastern parts of Tibet [65]. A dendroclimatological study of *Picea obovata* indicated that the latitudinal gradient also influences the response to a changing climate, and this influence can be significant between species and sites [66].

Several studies conducted in Pakistan have used tree growth data as a proxy for dates in studying variability in the past climate and to quantify the impact of climate on radial growth [67–74]. Spruce and fir are important coniferous tree species that are found in Pakistan's moist and dry temperate forest of the northern Himalayas [74,75]. Despite its significant dendroclimatological potential, very little is currently known about the relationship between climatic factors and the tree-rings of spruce and fir in Pakistan. Several studies conducted in Northern Pakistan have investigated the dendrochronology of spruce and fir. However, these studies primarily focused on a single location or single tree species, and studies regarding the responses of multiple species at various locations or spatial distributions along latitudinal gradients remain rare.

Furthermore, there are few studies that consider the influence of latitudinal gradients together with long-term growth trends resulting from rapidly warming and drying climatic conditions. From the perspectives of climate change and global warming, it is critical to improve our knowledge of the growth–climate relationships of spruce and fir in order to assess variability at various spatial and temporal scales. Therefore, this research comprises a regional dendroecological analysis of spruce and fir trees at five different sites in the

northern area of Pakistan along the latitudinal gradient. The main objectives of the study are: (1) to investigate the significant climatic factors affecting the radial growth of spruce and fir pine trees at five ecological sites; and (2) to develop a relationship between the latitudinal gradient and the growth–climate response of spruce and fir.

2. Methods

2.1. Study Site and Sample Collection

The study area for this research is in Northern Pakistan, comprising five study sites, namely, Shogran (SHG), Upper Dir (UDS), Bahrain Swat (BSG), Astore Gilgit (NPKA), and Sharan Kaghan (SHA). The study sites were selected at different locations in order to cover all representative forests of spruce and fir; the geographic coordinates of the five study sites are SHG: 73°29'10" E; 34°38'30" N; UDS: 72°02'30" E; 35°17'30" N; BSG: 72°34'30" E; 35°12'30" N; NPKA: 74°59'20" E; 35°34'10" N; and SHA: 73°25'50" E; 34°41'30" N (Table 1). The UDS and NPKA sites are in dry temperate forests and cover an altitudinal range of 2950 to 3600 m, whereas the SHG, BSG, and SHA sites are in moist temperate forests and cover an altitudinal range of 1830 to 2950 m, as shown in Figure 1 (Table 1). This research focused on the dendroclimatological study of two coniferous species of spruce and fir found in Northern Pakistan. Other associated trees species included *Cedrus deodara* (deodar) (Roxb.) Loud., *Pinus wallichiana* (kail) A. B. Jacks., 1938, *Pinus gerardiana* (chilgoza pine) Wall., *Taxus baccata* (taxus) L., *Salix tetrasperma* (willow) Roxb., *Quercus ilex* (quercus) Andr., and *Betula utilis* (birch) D. Don. The UDS and NPKA forests receive less rainfall than the SHG, BDG, and SHA forests, which receive more rainfall during the monsoon season (June to September in Northern Pakistan). Overall, the climates of the study sites are dry in the high-altitude areas and become progressively more humid at lower altitudes. The areas are characterized by four distinct seasons (winter, spring, summer, and autumn). June is considered the hottest month (before the monsoon), with a mean temperature range from 12 °C at a higher altitude to 16 °C at lower elevations (a microclimate exists in the northern aspects). In January, however, the temperature falls to between 4 and 2 °C as the winter season starts. Similarly, monsoon rainfall ranges from 1000 to 1350 mm at locations in the moist temperate forests of the SHG, BSG, and SHA sites (Figures 2 and 3).

Table 1. Details of sampling sites with elevations of spruce and fir at five sites (SHG, UDS, BSG, NPKA, SHA) during different periods.

Sampling Site	Latitude	Longitude	Forest Type	Elevation Range (Meter)
Shogran (SHG)	34°38'30" N	73°29'10" E	Moist Temperate Forests	1830 to 2950
Upper Dir (UDS)	35°17'30" N	72°02'30" E	Dry Temperate Forests	2950 to 3600
Bahrain Swat (BSG)	35°12'30" N	72°34'30" E	Moist Temperate Forests	1830 to 2950
Astore Gilgit (NPKA)	35°34'10" N	74°59'20" E	Dry Temperate Forests	2950 to 3600
Sharan Kaghan (SHA)	34°41'30" N	73°25'50" E	Moist Temperate Forests	2950 to 3600

2.2. Tree-Ring Data and Chronology Development

Spruce and fir tree-ring samples were collected from five sites in Northern Pakistan, which extend across a range of altitudinal (from 1415 to 3600 m) and latitudinal gradients (34° 38" to 35° 35" N) (Figure 1). We collected 27 (SHG), 30 (UDS), and 40 (BSG) tree core samples from 113 *Picea smithiana* (Wall.) Boiss. trees, and 23 (SHG), 25 (UDS), 28 (BSG), 20 (NPKA), and 26 (SHA) tree core samples from 140 *Abies pindrow* (Royle ex D. Don) Royle trees, from the five different sites in Northern Pakistan (Figure 1). The law prohibits all human interference in these forests; thus, the forests in the research region are protected by the forest department and are essentially free from human pressure. Samples were collected from coniferous forests with a uniform spatial distribution covering all representative forests of spruce and fir in Northern Pakistan. The collection of tree samples was completed in three different periods, i.e., 2005, 2017 and 2018. An increment borer was used to extract

the cores from each sampled tree of spruce and fir at a height of 1.3 m. One or two cores were extracted from the best (selected) trees among the codominant and dominant trees of both species in each site. All cores were safely wrapped in straw, transported from Pakistan to China, and stored in a laboratory. First, the cores were mounted with white glue and fixed with thread in wooden core mounts. The cores were dried for several days and polished to ensure the tree-rings were perfectly clear for unambiguous cross-dating. The tree-ring cores were cross-dated using the skeleton plot method (Stokes and Smiley, 1968), which graphically represents the annual tree-ring width pattern. Skeleton plots are easily interpreted and compared with the master tree-ring chronology of all the samples. The Velmex measurement system was used to measure the width of tree-rings with a minor count (precision) of up to 0.001 mm (Velmex, Bloomfield, NY, USA).

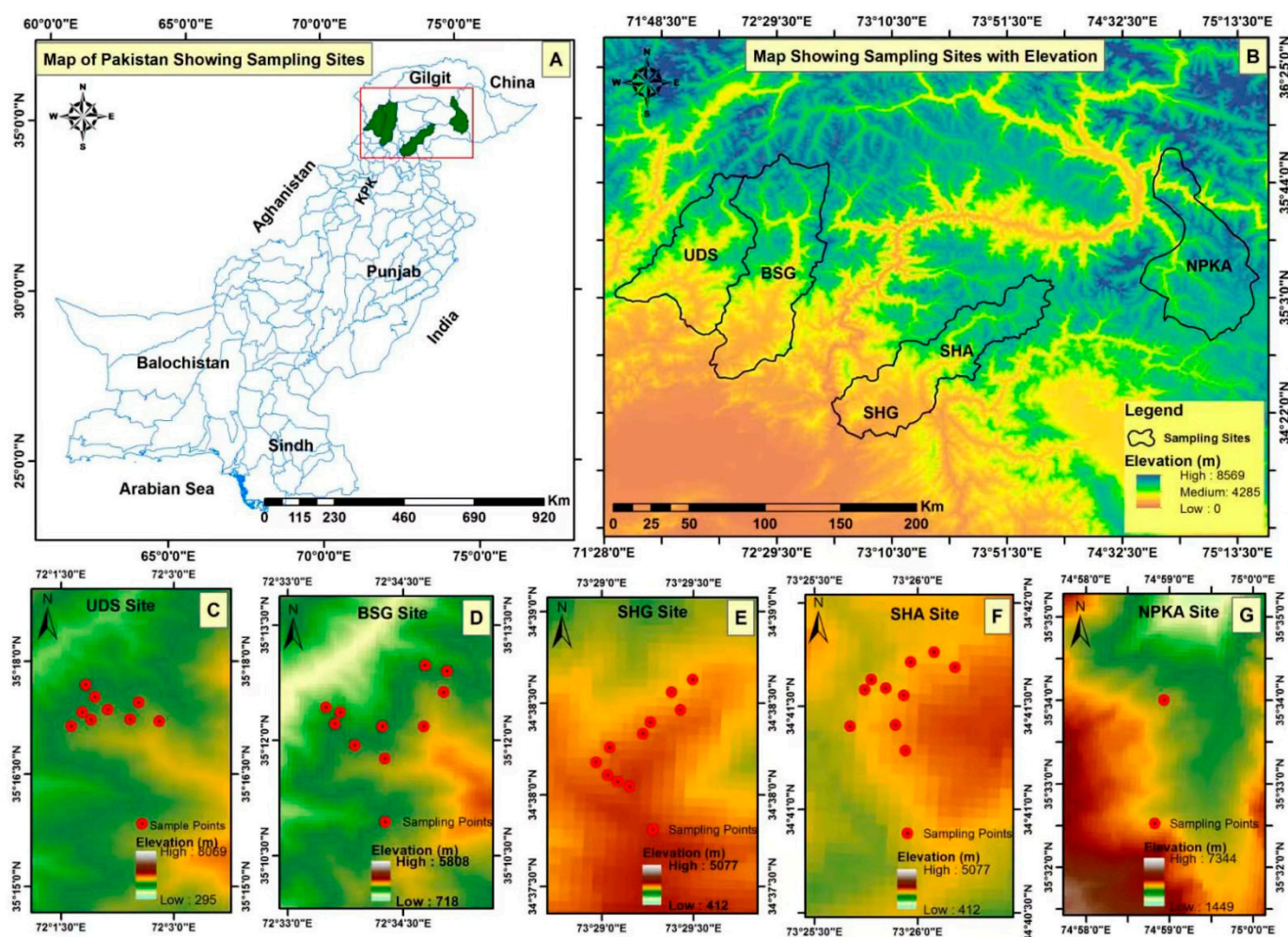


Figure 1. Map showing the study sites and elevation in Northern Pakistan. (A) Map of the Pakistan showing sampling sites, (B) Map showing sampling sites with elevation, (C) UDS site, (D) BSG site, (E) SHG site, (F) SHA site, and (G) NPKA site. The red circle shows sampling sites.

The COFFECHA program was used to check the quality of tree-ring measurement and the exact date of ring formation for each core, termed cross-dating [76,77]. Ring samples of the same tree species collected from different sites can be cross-dated by matching annual rings between the different cores. This method also ensures that the same calendar year is used for each annual ring and, thus, mistakes in measurement can be quickly eliminated. Tree-ring series were detrended and standardized using the ARSTAN program, which generates chronologies with minimal influence due to disturbances within a stand of spruce and fir. The ARSTAN program fitted negative exponential models to detrend growth trends

and nonclimatic signals. The correlation coefficient matrix of standard chronologies of spruce and fir at five sites from 1950 to 2018 is presented in Table 2. Different statistical characteristics of the standard chronologies are summarized in Table 3; these include first-order autocorrelation (AC1), standard deviation (SD), signal-to-noise ratio (SNR), mean sensitivity (MS), mean correlation of all series (MCC), expressed population signal (EPS), and variation in the first eigenvector (VAR). Correlation matrices were developed for both species covering 69 years (1950–2018) and summarized.

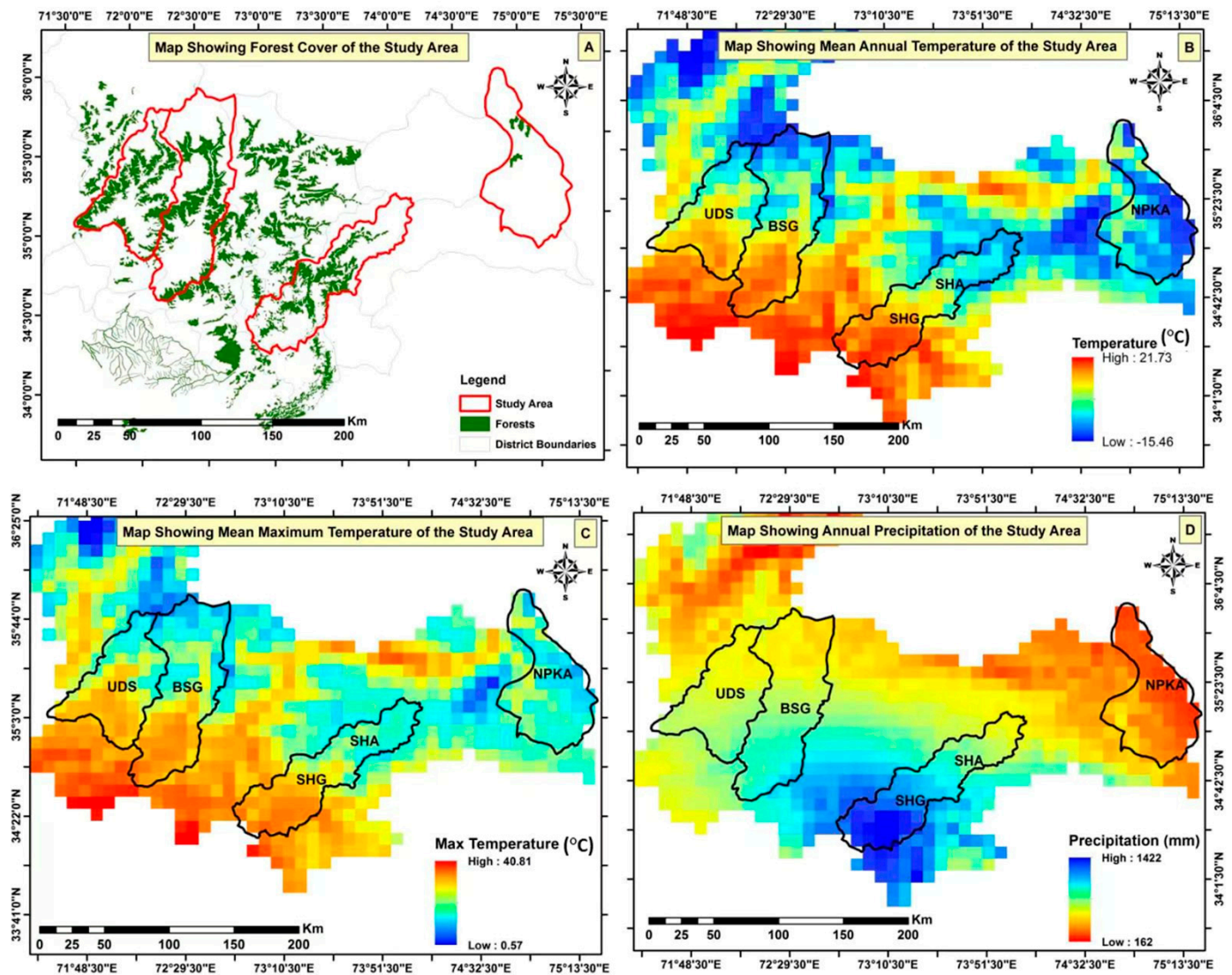


Figure 2. Map showing forest area, mean annual and maximum temperature, and precipitation of the study sites. (A) Map showing forest cover of the study area, (B) Map showing mean annual temperature of the study area, (C) Map showing mean maximum temperature of the study, and (D) map showing annual precipitation of the study area.

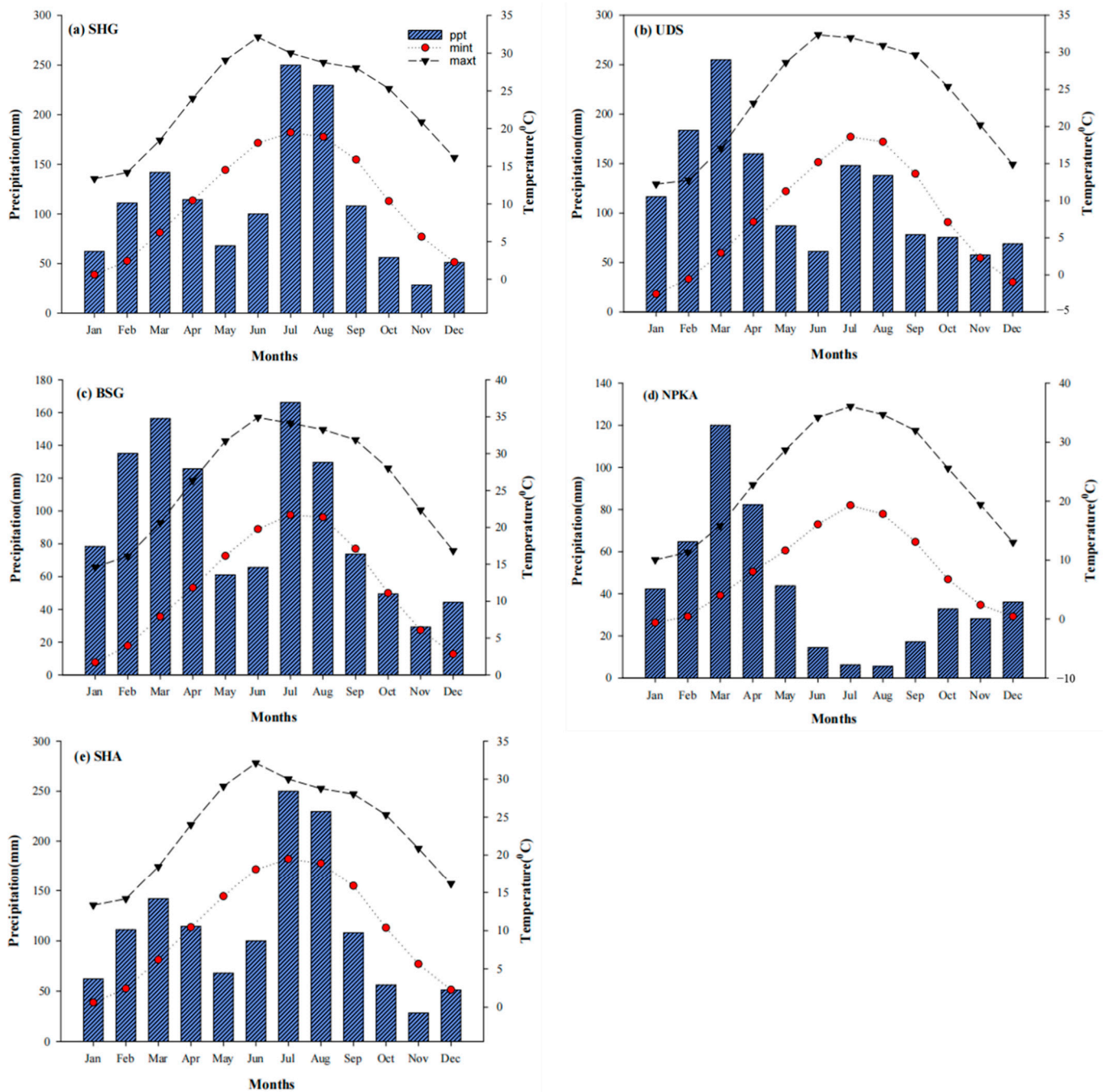


Figure 3. Study area showing sampling sites, meteorological stations, and scPDSI grid points. (a–e) shows different sampling sites (a) SHG, (b) UDS, (c) BSG, (d) NPKA, and (e) SHA.

Table 2. Correlation coefficient matrix of standard chronologies of spruce (SP) and fir (F) at five sites (SHG, UDS, BSG, NPKA, SHA) during different periods.

	SHGSP	UDSSP	BSGSP	SHGF	UDSF	BSGF	NPKAF	SHAF
SHGSP	1	0.281 **	0.200 **	0.447 **	0.286 **	−0.142	0.262 **	0.458 **
UDSSP	0.281 **	1	0.164 *	0.164 *	0.579 **	0.050	0.162 *	0.400 **
BSGSP	0.200 **	0.164 *	1	0.288 **	0.179 *	0.114	−0.068	0.021
SHGF	0.447 **	0.164 *	0.288 **	1	0.337 **	0.002	0.169 *	0.516 **
UDSF	0.286 **	0.579 **	0.179 *	0.337 **	1	0.103	0.101	0.369 **

Table 2. *Cont.*

	SHGSP	UDSSP	BSGSP	SHGF	UDSF	BSGF	NPKAF	SHAF
BSGF	−0.142	0.050	0.114	0.002	0.103	1	−0.117	−0.167 *
NPKAF	0.262 **	0.162 *	−0.068	0.169 *	0.101	−0.117	1	0.295 **
SHAF	0.458 **	0.400 **	0.021	0.516 **	0.369 **	−0.167 *	0.295 **	1

** . Correlation is significant at the 0.01 level (two-tailed). * . Correlation is significant at the 0.05 level (two-tailed).

Table 3. Statistical characteristics of spruce and fir standard chronologies at five sites (SHG, UDS, BSG, NPKA, SHA) of the northern area of Pakistan.

	<i>Picea smithiana</i>			<i>Abies pindrow</i>				
	SHG	UDS	BSG	SHG	UDS	BSG	NPKA	SHA
TS	1850–2017	1804–2017	1842–2018	1806–2017	1835–2017	1851–2018	1505–2005	1696–2018
TN	27(34)	30(34)	40(45)	23(30)	25(30)	28(34)	20(25)	26(30)
MRW (mm)	0.9746	0.9798	0.9931	0.9763	0.958	0.9755	0.987	0.9725
MS	0.1182	0.2132	0.1122	0.143	0.1645	0.1608	0.1449	0.1458
SD	0.1434	0.2993	0.1587	0.1848	0.1952	0.1883	0.1449	0.2981
AC1	0.5165	0.4938	0.6	0.5696	0.4501	0.4929	0.4528	0.7962
ISC	0.449	0.559	0.494	0.547	0.495	0.524	0.608	0.481
Common Interval Analysis for Period 1891 to 2018								
Var	24.85%	34.66%	19.28%	27.88%	29.21%	25.45%	33.64%	36.01%
SNR	5.405	8.416	5.101	6.285	6.134	5.701	7.238	8.732
EPS	0.844	0.894	0.836	0.863	0.86	0.851	0.879	0.897
MCC	0.197	0.277	0.116	0.222	0.235	0.186	0.266	0.294

Notes: TS—time span, TN—tree (core) number, MRW—mean ring width, MS—mean sensitivity, SD—standard deviation, AC1—first-order autocorrelation, ISC—interseries correlation, Var—variation in the first eigenvector, SNR—signal-to-noise ratio, EPS—expressed population signal, MCC—mean correlation coefficients among all sites.

2.3. Climatic Data and Statistical Analysis

Only 30 years of climate data were available in meteorological stations located near the study sites (SHG, UDS, BSG, NPKA, and SHA), whereas the present study required climate data for 69 years (from 1950 to 2018). Therefore, climate data were downloaded from KNMI Climate Explorer (<https://climexp.knmi.nl>, accessed on 15 November 2018) [37], which contains a gridded dataset of monthly mean temperature and total precipitation known as CRU TS 4.01 (<http://www.cru.uea.ac.uk/cru/data/hrg.htm>, accessed on 15 November 2018) [37]. These data have been checked for quality and aggregated to a larger spatial scale; thus, these gridded climate datasets are frequently more reliable than individual station data [37]. We downloaded monthly data covering mean temperature, minimum temperature, and maximum temperature for 1901–2019, but used only a subset of the data, i.e., 1950–2018. In order to quantify the relationship between tree-ring width and long-term drought in the latitude of Pakistan (low latitudes), we also downloaded the extensively used Palmer Drought Severity Index (PDSI) from KNMI Climate Explorer [78]. We used the CRU scPDSI 3.26e product to estimate dryness from existing temperature and precipitation datasets. PDSI better indicates variations in potential evapotranspiration by integrating physical water balance and air temperature. The relationship between monthly climate data and the radial growth of spruce and fir was assessed using the Pearson correlation. The relationships between radial growth (chronologies) and seasonal climate data were determined by analyzing the differences in correlation, representing the stability of the dendroclimatological relationships in the whole range. The seasonal climate was split into four different seasons: winter (December to February), spring (March

to May), summer (June to August), and autumn (September to November). In addition, the dendroclimatological relationships of spruce and fir were examined in two periods: prior to rapid warming (i.e., before 1980), and following rapid warming (after 1980). SPSS (SPSS version 26.0, Chicago, IL, USA) software was used for statistical analyses [79,80].

3. Results

3.1. Tree-Ring Width Chronologies

Three long-term tree-ring chronologies were developed for spruce, including one of 167 years (AD 1850–2017) at SHG, one of 213 years (AD 1804–2017) at UDS, and one of 176 years (AD 1842–2018) at BSG (Table 3). Similarly, for *Abies pindrow*, five long-term tree-ring chronologies were developed, including one of 211 years (AD 1806–2017) at SHG, one of 182 years (AD 1835–2017) at UDS, one of 167 years (AD 1851–2018) at BSG, one of 500 years (AD 1505–2005) at NPKA, and finally one of 322 years (AD 1696–2017) at SHA (Table 3). In the case of *Abies pindrow*, the age of 80/122 samples exceeded 100 years, of which 22, 12, 13, 20, and 13 samples were collected from SHG, UDS, BSG, NPKA, and SHA, respectively. Similarly, in the case of *Picea smithiana*, 43/97 samples surpassed 100 years, of which 13, 12, and 18 samples were collected from SHG, UDS, and BSG, respectively (Table 3). The average age of the firs at the different sites was 157.1 years at SHG, 122.8 years at UDS, 106.7 years at BSG, 325.9 years at NPKA, and 238.9 years at SHA. On the other hand, the mean ages of the spruce were 98.1, 101.4, and 100.5 years for SHG, UDS, and BSG, respectively. The greatest fir tree longevity was found in NPKA, with 8 samples exceeding 400 years, 2 samples exceeding 300 years, and 8 samples exceeding 200 years. The SHA location also reflected the high longevity of fir trees, with 3 samples exceeding 300 years and 17 samples surpassing 200 years. The interseries correlation of both species showed that the stand signal and dating were good quality. The interseries correlations for fir were 0.547, 0.495, 0.524, 0.608, and 0.481 for SHG, UDS, BSG, NPKA, and SHA, respectively. For *Picea smithiana*, the interseries correlations were 0.449 for SHG, 0.559 for UDS, and 0.494 for BSG. The mean sensitivity values for both species showed that the tree rings could indicate minor climatic changes within the specified period. For *Abies pindrow*, the mean sensitivity values were 0.143, 0.164, 0.160, 0.144, and 0.145 at SHG, UDS, BSG, NPKA, and SHA respectively. Similarly, in *Picea smithiana*, the mean sensitivity values were 0.118 at SHG, 0.213 at UDS, and 0.112 at BSG (Table 3).

Growth variability in spruce samples was observed between 1850 and 2018 (Figure 4a). The lowest tree-ring width was 0.54 in 1879, the most severe drought year of the studied period, whereas the highest was 1.42 in 1854, which indicated the most humid year with the highest cambium growth of spruce at the SHG site. Other prominent drought years were 1918, 1921, 1947, 1985, and 2017 with tree-ring widths of 0.60, 0.65, 0.66, 0.72, and 0.79, respectively. Prominent humid years were 1851, 1855, 1874, 1886, 1938, 2003, and 2005, with corresponding tree-ring widths of 1.33, 1.36, 1.21, 1.15, 1.20, 1.32, 1.21, 1.22, and 1.22, respectively. The highest climate variability was recorded in two periods, the first between 1850 and 1892, and the second between 1985 and 2017, whereas the lowest climate variability was found in the periods 1899–1910 and 1963–1977.

Growth variability was also identified in spruce samples collected from UDS (Figure 4b). The lowest tree-ring width was 0.40 in 1892, the most severe drought year, whereas the highest was 2.32 in 1822, which indicates the most humid year with the highest cambium growth. Other prominent drought years were 1815, 1840, and 1835, with tree-ring widths of 0.47, 0.44, and 0.46, respectively. Prominent humid years were 1818, 1814, and 1827 with corresponding tree-ring widths of 2.23, 2.09, and 1.92, respectively. The highest climate variability was recorded in two periods, the first between 1804 and 1843, and the second between 1872 and 1900, whereas the lowest climate variability was found in the period 1915–1991. Compared to UDS and SHG, greater variability was observed in BSG (Figure 4c). The results showed that the lowest tree-ring width was 0.60 in 1879, which was the most severe drought year, whereas the highest was 1.47 in 1861, which indicates the most humid year with the highest cambium growth. Other prominent drought years

were 1908, 1923, 1979, 2001, and 2012 with tree-ring widths of 0.63, 0.64, 0.72, 0.75, and 0.75, respectively. Prominent humid years were 1862, 1860, 1863, and 1856 with corresponding tree-ring widths of 1.41, 1.36, 1.34, and 1.29, respectively. The highest climate variability was recorded in two periods, the first between 1842 and 1879, and the second between 1997 and 2018, whereas the lowest was found in the period 1951–1981.

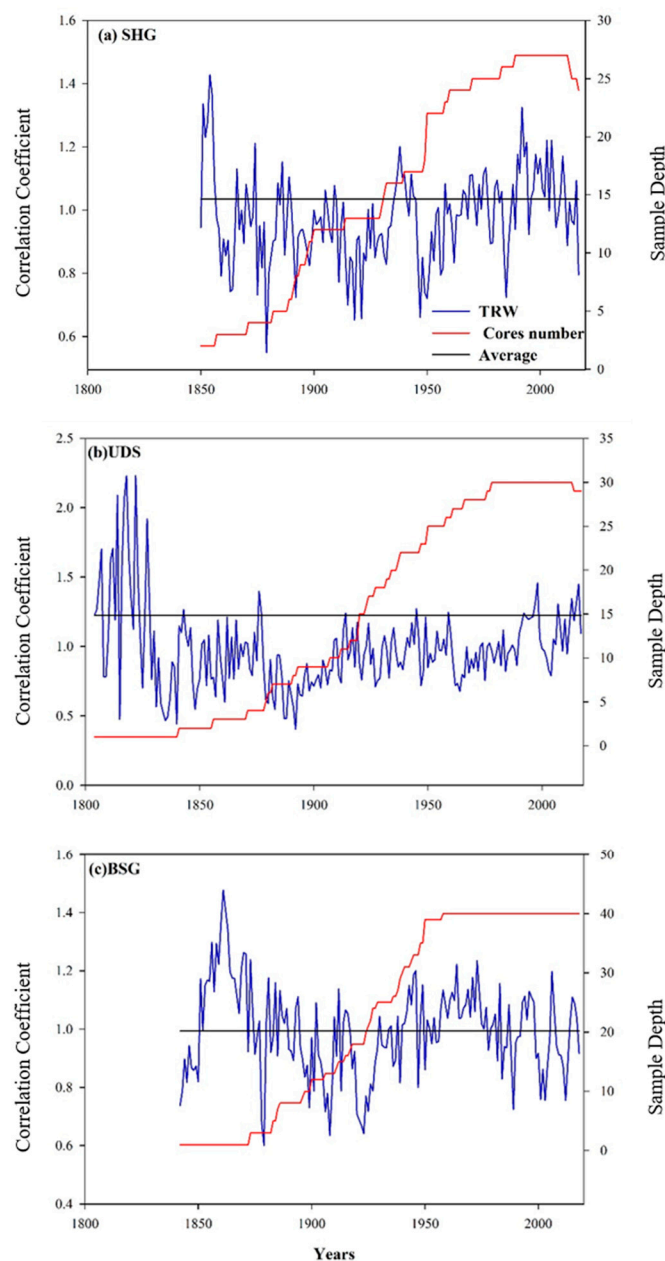


Figure 4. Standard tree ring chronologies of spruce (a–c) during the period 1800–2018 at SHG, UDS, and BSG in the northern area of Pakistan.

The lowest tree-ring width for fir at SHG (Figure 5a) was 0.58 in 1928, which was the most severe drought year, whereas the highest was 1.52 in 1972, which was the most humid year with the highest cambium growth. Other prominent drought years were 0.61, 0.61, 0.24, 0.59, and 0.60 in 1825, 1831, 1879, 1928, and 1947, respectively. Prominent humid years were 1819, 1872, 1964, and 1997, with corresponding tree-ring widths of 1.38, 1.34, 1.45, and 1.43, respectively. The highest climate variability was recorded in two periods, the first between 1819 and 1879, and the second between 1986 and 2017, whereas the lowest

was found in the period 1903–1952. Similarly, at UDS (Figure 5b), the highest climate variability was recorded between 1882 and 2017, whereas the lowest was found in the periods 1882–2017, 1893–1913, and 1935–1956 with respect to *Abies pindrow* radial growth. However, for fir at the BSG site (Figure 5c), the lowest tree-ring width was 0.52 in 1982, which was the most severe drought year, whereas the highest was 1.62 in 1931, the most humid year. The highest climate variability was recorded between 1943 and 1982, whereas the lowest was found between 1863 and 1988 (Figure 5c). Similarly, the highest climate variability in fir growth was recorded in the period between 1952 and 2018, whereas the lowest climate variability was found between 1879 and 1956 at the SHA site (Figure 5d). At the NPKA site (Figure 5e), the highest climate variability was recorded in the period between 1505 and 1574, whereas the lowest climate variability was found between 1881 and 1970.

3.2. Growth–Climate Relationship

The correlation between the tree-ring width of both species and monthly precipitation is summarized in Figure 6a–e. For spruce at SHG, a significant positive correlation was observed only in January ($R^2 = 0.39$) with p -value ≤ 0.05 . In comparison, no correlation was found between fir tree-ring width and precipitation at SHG. Similarly, at the UDS sampling site, spruce tree-ring widths were significantly positively correlated with precipitation in April ($R^2 = 0.37$) and May ($R^2 = 0.39$), with p -values of 0.05 and 0.01, respectively. In the case of fir, tree-ring widths showed a negative correlation with precipitation in December ($R^2 = 0.36$), followed by a positive correlation in April ($R^2 = 0.37$) and May ($R^2 = 0.39$) with a 0.05 significance level.

With respect to the BSG site, precipitation in October and March positively correlated with spruce tree-ring widths ($R^2 = 0.28$ and 0.35 , respectively); however, a negative correlation was observed in July ($R^2 = 0.37$) with a p -value of 0.05. Similarly, in the case of fir, tree-ring widths had a strong negative correlation ($R^2 = 0.37$) with precipitation in September. However, no relationship existed between the tree-ring widths of fir and monthly precipitation at the NPKA and SHA sites, which indicates that the tree-ring widths of the sampled trees were not influenced by monthly precipitation.

With respect to PDSI at the SHG site, the tree-ring widths of spruce showed no correlation, whereas fir had a good positive correlation with PDSI in April ($R^2 = 0.35$), May ($R^2 = 0.37$), June ($R^2 = 0.39$), and July ($R^2 = 0.35$) (Figure 7a–e). At the UDS site, the growth of fir and spruce had a very similar relationship with the corresponding PDSI. The results showed that both species had a strong positive correlation ($R^2 = 0.39$) with PDSI in October, April, May, June, July, August, and September. Moreover, the growth of spruce had a good correlation with PDSI in January ($R^2 = 0.39$), February ($R^2 = 0.39$), and March ($R^2 = 0.38$). At BSG, tree-ring widths showed a strong positive correlation in October ($R^2 = 0.38, 0.39$), the prior November ($R^2 = 0.36, 0.39$), April ($R^2 = 0.37, 0.39$), July ($R^2 = 0.36, 0.39$), and August ($R^2 = 0.35, 0.39$) for spruce and fir, respectively. However, a more significant influence of PDSI was observed on the growth of fir compared to spruce. Furthermore, significant positive relationships with PDSI existed in other months, i.e., in January, February, and March for *Picea smithiana*, and in May and June in the case of *Abies pindrow*. In contrast, a negative correlation ($R^2 = 0.38$) was observed between the growth of fir and PDSI in May at the NPKA site, whereas a nonsignificant correlation was observed for the same species at the SHA site. Overall, PDSI had a greater influence on the growth of fir in the summer and autumn seasons at the SHG, UDS, and BSG sites, whereas it had noticeable effects on spruce in the spring and autumn seasons at the UDS and BSG sites.

The correlation between the monthly mean temperature and tree-ring width of spruce and fir is presented in Figure 8a–e. The results show that the mean annual temperature had less influence on the growth of both species compared to annual precipitation and monthly PDSI. At the SHG site, spruce growth did not correlate with temperature, whereas the growth of fir had a negative correlation ($R^2 = 0.37$) with the mean annual temperature in May. Similarly, there was a nonsignificant correlation between the tree-ring width of both

species at the UDS site with annual mean temperature. Similarly, at the BSG site, the tree-ring width of spruce had a positive correlation with the February mean annual temperature ($R^2 = 0.37$), whereas the growth of fir showed no relationship with the temperature at the same site. However, strong positive correlations ($R^2 = 0.35, 0.39$, and 0.39) were observed at the SHA site in the growth of fir during December, January, and August, respectively. In contrast, no relationship existed between the mean annual temperature and tree-ring widths of fir at the NPKA site.

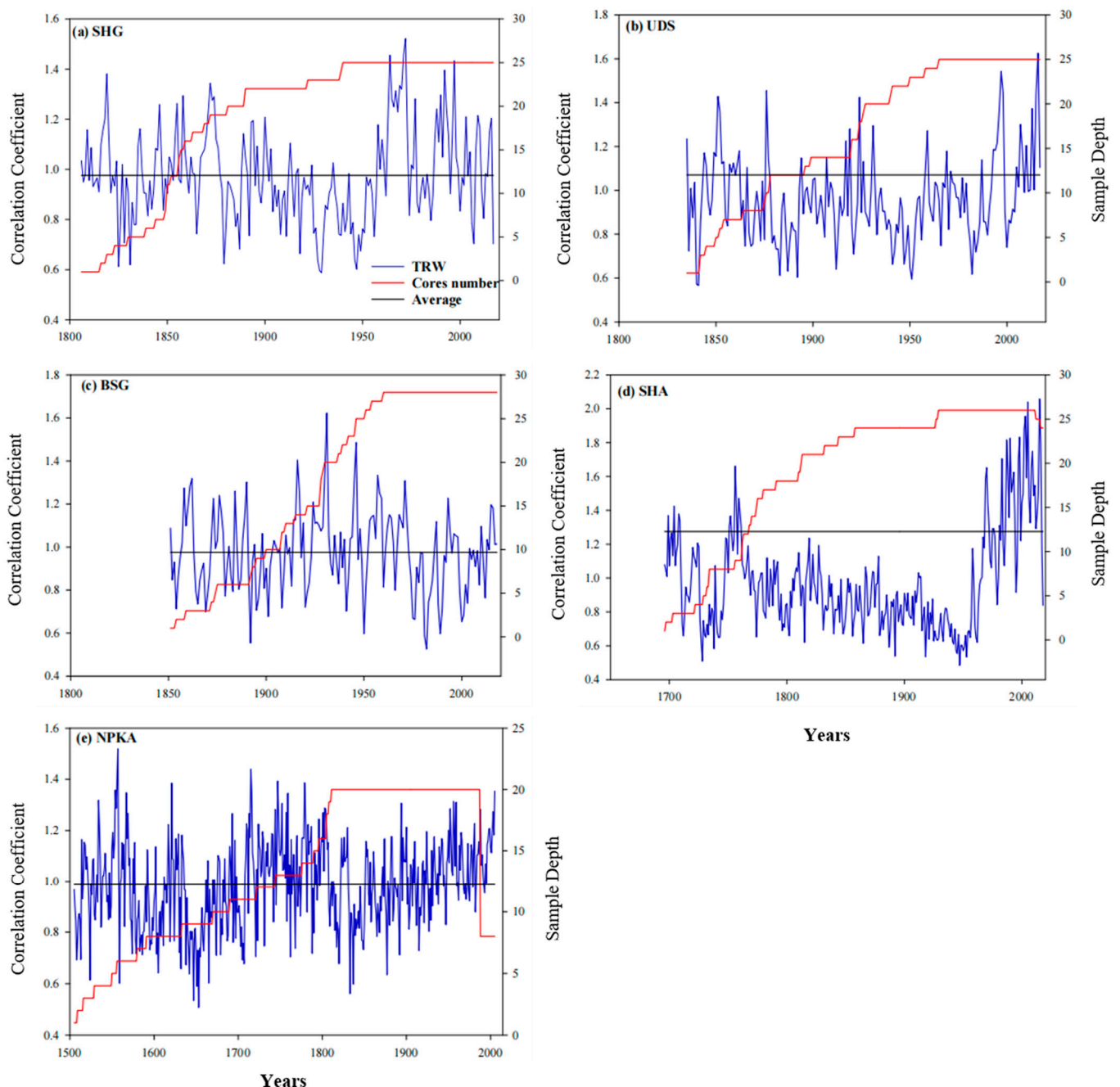


Figure 5. Standard tree ring chronologies of spruce and fir (a–e) during 1800–2018 at SHG, UDS, BSG, SHA, and NPKA in the northern area of Pakistan.

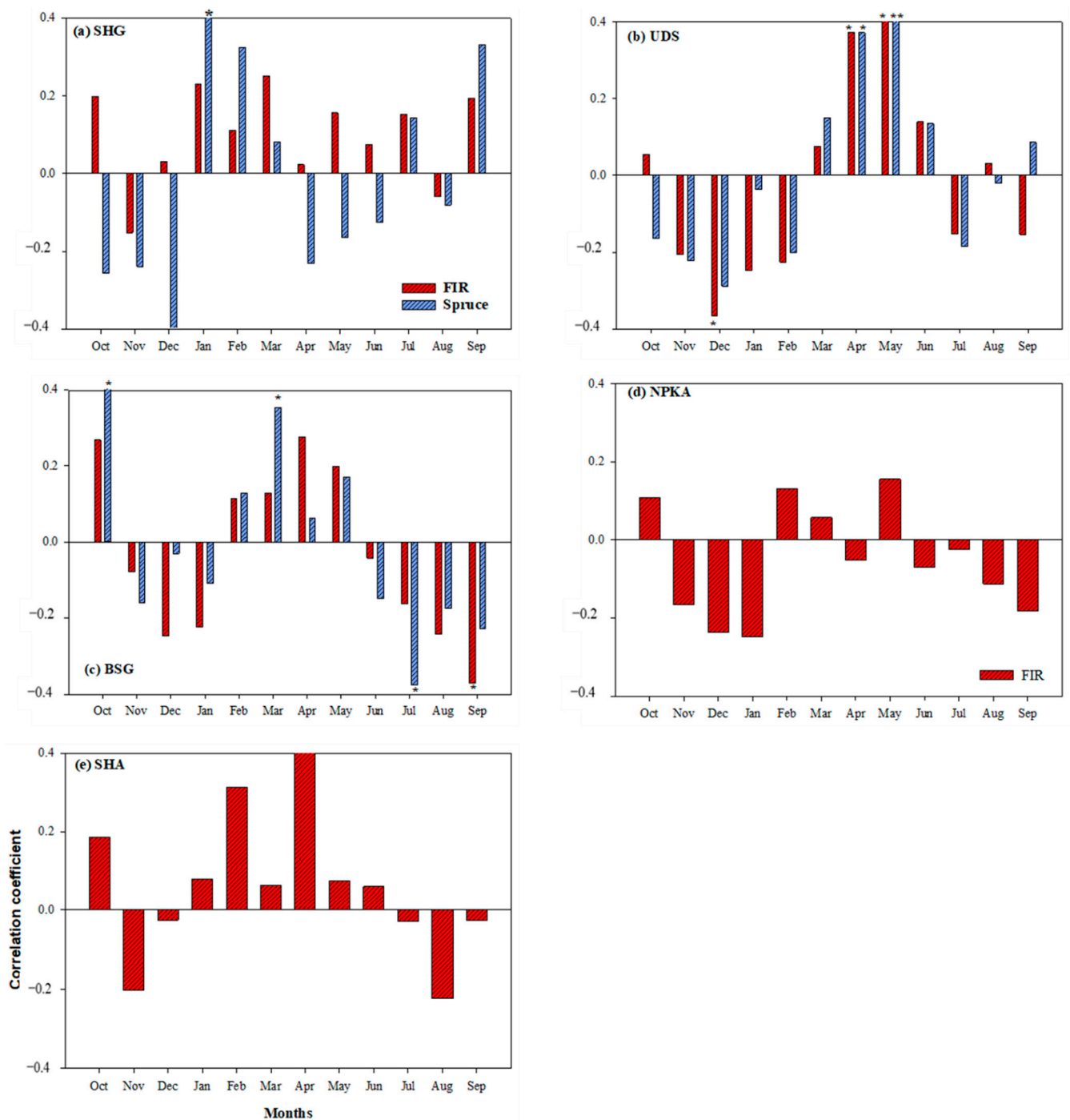


Figure 6. (a–e). Response function analysis between the tree-ring chronology of spruce (blue bar) and fir (red bar) and monthly total precipitation (a–e) during the period 1950–2018 at five sites (SHG, UDS, BSG, NPKA, and SHA) in Northern Pakistan. Stars indicate a significance level of $p < 0.01$.

3.3. Dendroclimatological Relationship before and after Rapid Warming

Over the last century, the temperature in Northern Pakistan has progressively increased, as reported by Bukhari and Bajwa [10] and Shah et al. [81]. The results of the growth relationships of fir and spruce with seasonal PDSI show an increased correlation after warming (Table 4). At the SHG site, spruce showed a negative correlation for the periods before and after 1980. The coefficient of correlation did not change significantly, which shows that seasonal PDSI had a minor effect on spruce growth. On the other hand, in the case of fir at the SHG site, the growth–seasonal PDSI relationships were negatively

correlated before 1980 and positively correlated after the 1980 warming period (Table 4). At the UDS site, the correlation of spruce increased from lower to higher values before and after 1980, respectively, in the spring, summer, and autumn seasons.

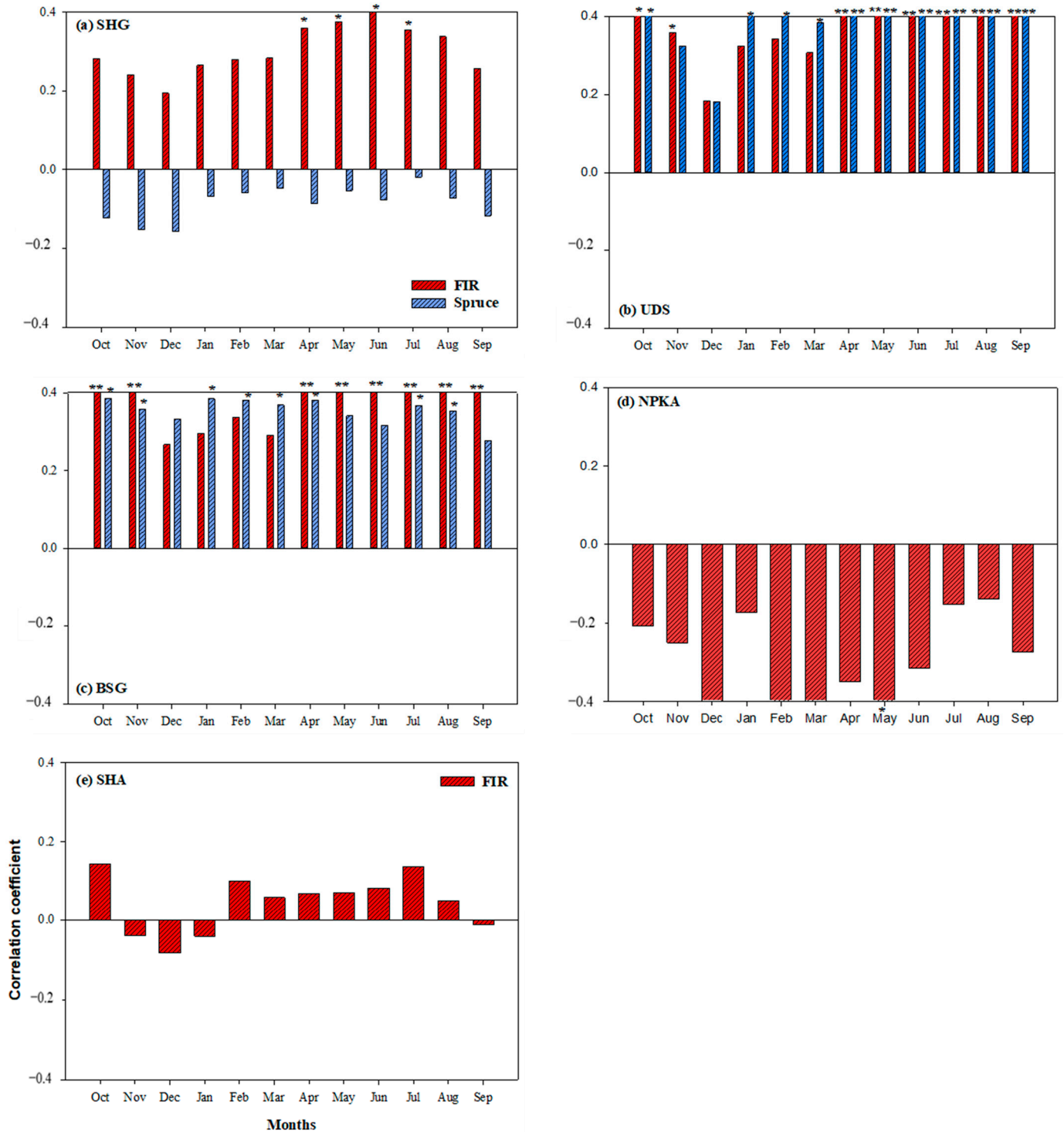


Figure 7. Response function analysis between the tree-ring chronology of spruce (blue bar) and fir (red bar) and PDSI (a–e) during the period 1950–2018 at five sites (SHG, UDS, BSG, NPKA, SHA) in Northern Pakistan. Stars indicate a significance level at $p < 0.01$.

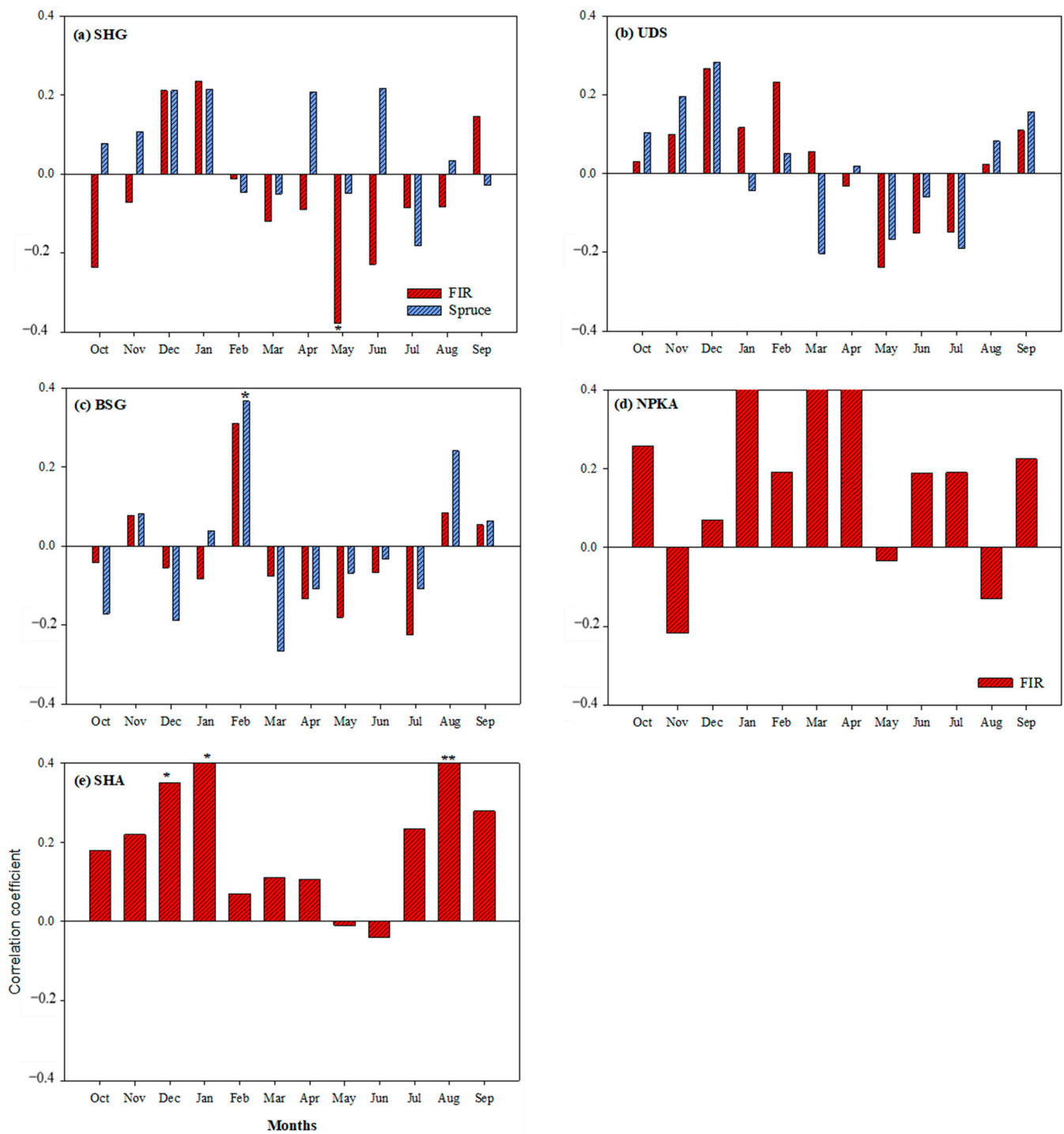


Figure 8. Response function analysis between the tree-ring-chronologies of spruce (blue bar) and fir (red bar) and mean annual temperature (a–e) during the period 1950–2018 at five sites (SHG, UDS, BSG, NPKA, and SHA) in Northern Pakistan. Stars indicate a significance level of $p < 0.01$.

Similarly, in regard to the growth–PDSI relationship for fir at the UDS site, the correlation increased in the summer and autumn but decreased in winter and spring before and after the 1980 warming period. Furthermore, at the BSG site, an increased correlation was observed for both species apart from *Abies pindrow* in the winter, which showed a slightly lower correlation after 1980. In the growth–PDSI relationship for spruce, the correlation changed from negative to positive when considering the period before and after 1980, respectively. At the NPKA site, fir growth increased but was negatively correlated

with PDSI before and after the warming period (1980). In contrast to NPKA, the correlation for fir growth at the SHA site decreased after 1980 apart from in the spring, when it remained unchanged.

Table 4. Correlation coefficients between seasonal PDSI and the tree-ring index of spruce and fir at five sites (SHG, UDS, BSG, NPKA, SHA) during 1950–1980 and 1981–2018.

		SHG		UDS		BSG		NPKA		SHA	
		1950–1980	1981–2017	1950–2017	1981–2017	1950–1980	1981–2018	1950–1980	1981–2005	1950–1980	1981–2017
<i>Picea smithiana</i>	pWinter	0.026	−0.019	0.393 *	0.316	0.051	0.362 *				
	Spring	−0.007	−0.013	0.269	0.388 *	−0.088	0.416 *				
	Summer	−0.119	0.043	0.208	0.454 **	−0.146	0.429 **				
	Autumn	−0.167	−0.037	0.253	0.352 *	−0.232	0.306				
<i>Abies pindrow</i>	pWinter	−0.128	0.325 *	0.247	0.205	0.265	0.227	−0.052	−0.419 *	−0.466 **	0.012
	Spring	−0.124	0.310	0.153	0.017	0.131	0.239	−0.032	−0.488 *	0.079	0.079
	Summer	−0.224	0.372 *	0.201	0.393 *	0.186	0.391 *	−0.265	−0.379	−0.413 *	0.143
	Autumn	−0.300	0.332 *	0.159	0.340 *	0.102	0.449 **	−0.273	−0.444 *	−0.454 *	0.042

** . Correlation is significant at the 0.01 level (two-tailed). * . Correlation is significant at the 0.05 level (two-tailed).

The relationships between seasonal precipitation and the tree-ring width of fir and spruce before and after rapid warming (1980) are presented in Table 5. The results show the correlation in a few seasons for both species, though the relationships were insignificant (Table 5). A significant association was found for fir in summer before 1980 (at SHG), in spring after 1980 (at UDS and BSG), and in the most recent winter after 1980 (at NPKA). *Picea smithiana*, on the other hand, demonstrated a statistically significant correlation in winter before 1980 and in spring after 1980 at UDS, but at BSG, a statistically significant correlation was observed in summer before 1980 and in spring after 1980. However, no significant relationship existed between the growth of spruce and seasonal precipitation before and after rapid warming (Table 5).

Table 5. Correlation coefficients between seasonal precipitation and the tree-ring index of spruce and fir at five sites (SHG, UDS, BSG, NPKA, SHA) during 1950–1980 and 1981–2018.

		SHG		UDS		BSG		NPKA		SHA	
		1950–1980	1981–2017	1950–2017	1981–2017	1950–1980	1981–2018	1950–1980	1981–2005	1950–1980	1981–2017
<i>Picea smithiana</i>	pWinter	−0.099	0.246	0.401 *	−0.077	0.142	0.000				
	Spring	−0.140	0.015	−0.087	0.437 **	−0.104	0.406 *				
	Summer	−0.075	0.040	−0.016	0.200	−0.379 *	0.120				
	Autumn	−0.103	0.114	0.274	−0.153	−0.056	−0.080				
<i>Abies pindrow</i>	pWinter	−0.004	0.044	0.130	−0.065	0.095	−0.023	0.058	−0.446 *	−0.149	0.168
	Spring	0.052	0.282	0.123	0.415 *	0.065	0.365 *	0.323	−0.275	0.168	0.186
	Summer	−0.380 *	0.145	−0.161	0.302	−0.312	0.262	−0.321	0.208	−0.049	−0.084
	Autumn	0.083	−0.032	0.136	−0.045	0.350	0.113	−0.134	−0.173	−0.131	−0.019

** . Correlation is significant at the 0.01 level (two-tailed). * . Correlation is significant at the 0.05 level (two-tailed).

3.4. Dendroclimatological Relationship with Latitude

Variations in the relationship of fir and spruce tree-ring width and seasonal temperature with increasing latitude are shown in Figure 9a–d. During the winter season (December–February), the correlation of fir growth and seasonal temperature showed an upward trend from 30° to 34° latitude and then a downward trend from 34° to 35° latitude (Figure 9a). Similarly, the correlation between spruce and seasonal temperature showed a downward trend up to 35° latitude and a gradual upward trend with increasing latitude thereafter (Figure 9a). In the spring season, the growth of both species showed an almost opposite trend from a lower (30°) to higher (35°) latitude (Figure 9b). During summer (June–August), the correlation between the growth of fir and seasonal temperature showed

a downward trend with increasing latitude (from 30° to 35°), whereas in the case of spruce, the correlation showed a downward trend from 30° to 32° latitude. The trend remained constant with increasing latitude (Figure 9c). During autumn (September–November), the correlation for fir showed no prominent trend (the curve was almost straight); however, the correlation for spruce showed an upward trend up to 32° latitude and then a downward trend beyond that latitude (Figure 9d).

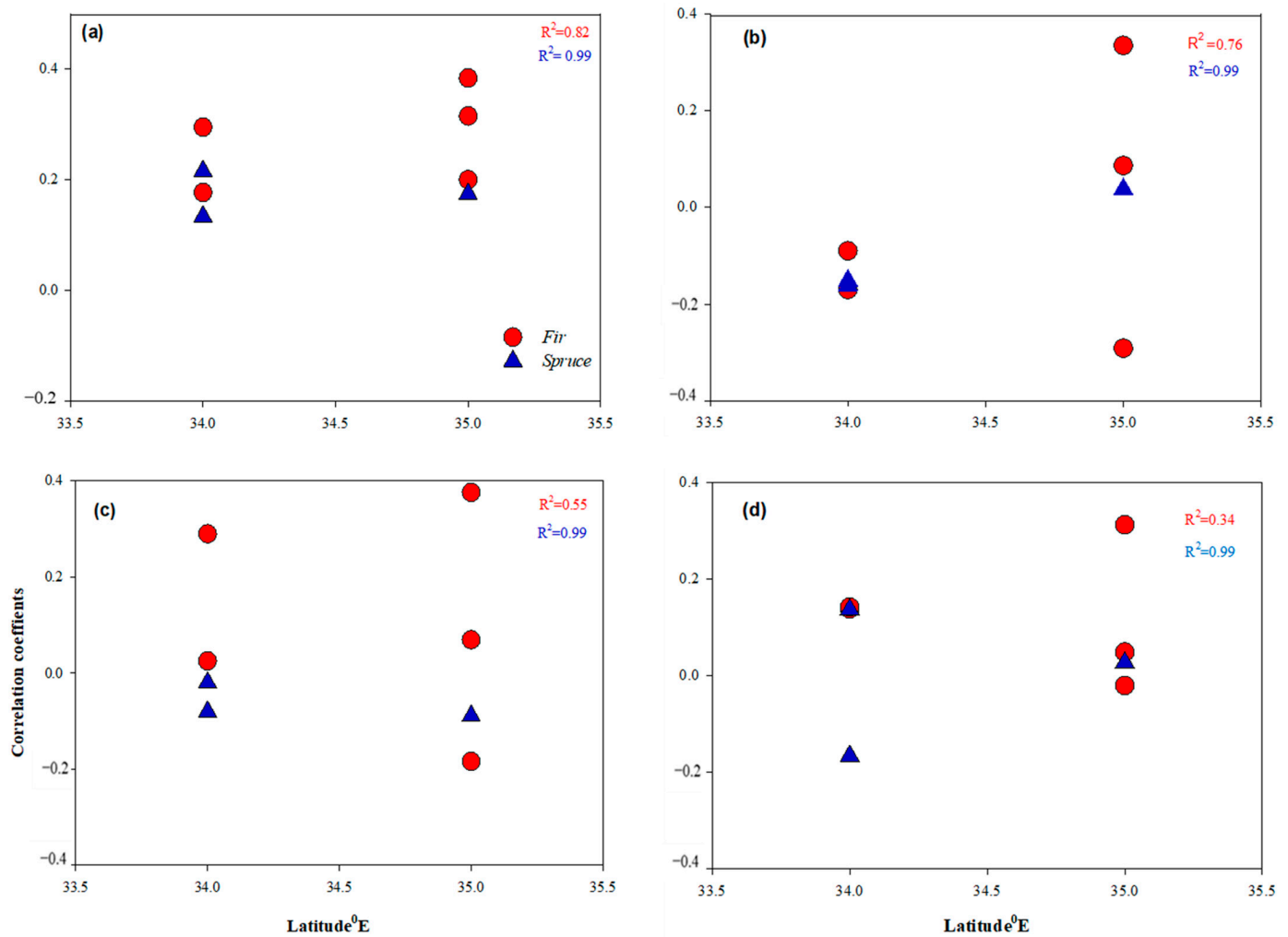


Figure 9. Variation of correlation coefficients between the tree-ring chronologies of spruce (blue triangles) and fir (red dots) and seasonal temperature with latitudes during 1950–2018. (a) Winter (Dec–Feb), (b) spring (Mar–May), (c) summer (Jun–Jul), and (d) autumn (Sep–Nov).

The correlation of fir and spruce and seasonal precipitation showed a positive upward trend from lower to higher latitudes (Figure 10a–d). In winter (December–February), the growth of fir initially showed a positive correlation (30–36°) followed by a slight downward trend of the curve with increasing latitude, whereas spruce showed an increasing trend with an increase in latitude. Both species showed an upward trend. In contrast, during summer (June–August), the correlation for both species showed a downward trend with increasing latitude. During autumn (September–November), both species showed the opposite trend with the increase in latitude (Figure 10a–d).

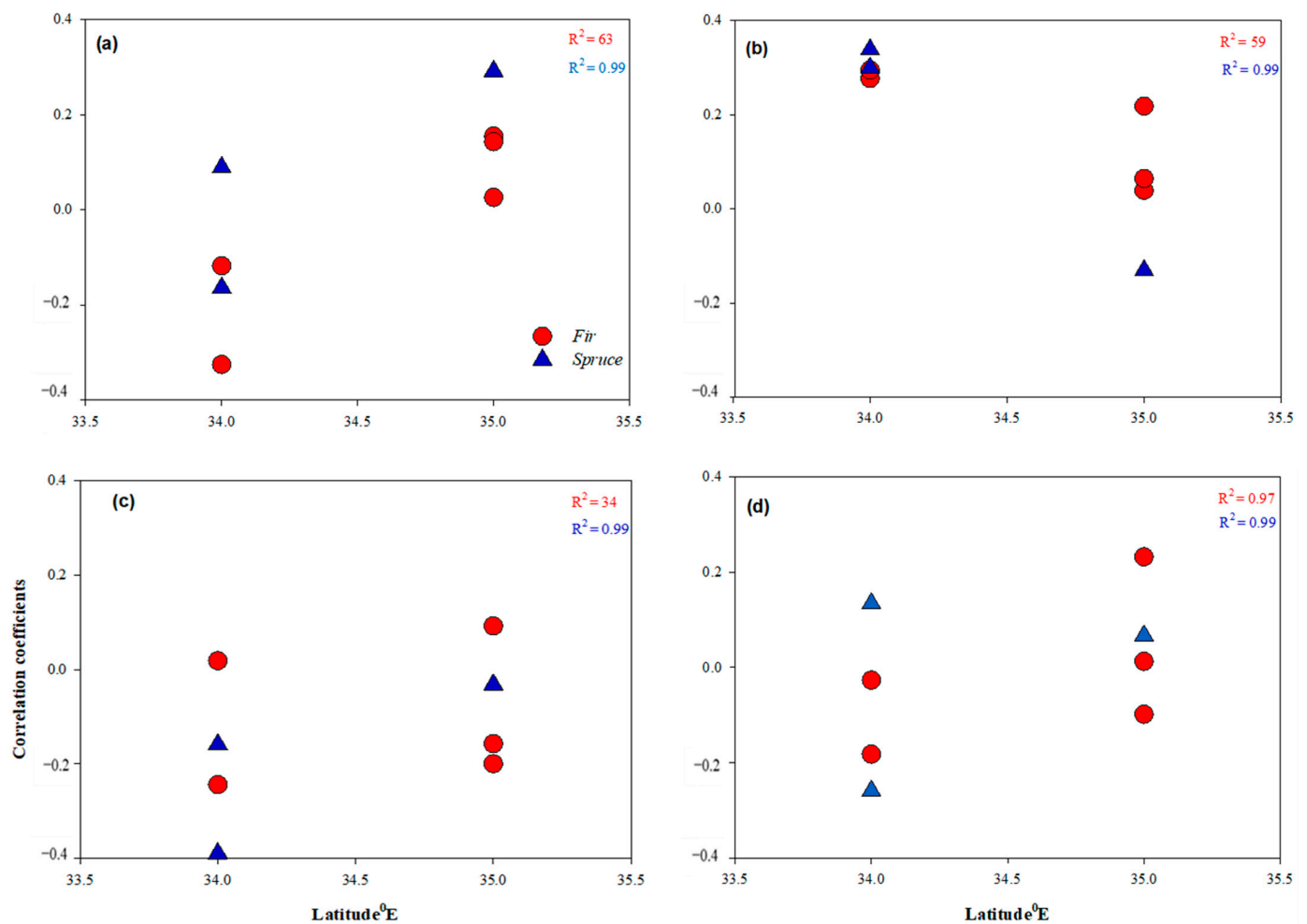


Figure 10. Variation of correlation coefficients between the tree-ring chronologies of spruce (blue triangles) and fir (red dots) and seasonal precipitation with latitudes during 1950–2018. (a) Winter (Dec–Feb), (b) spring (Mar–May), (c) summer (Jun–Jul), and (d) autumn (Sep–Nov).

The correlation of PDSI and the growth of fir and spruce with increasing latitude is shown in Figure 11. During the winter, summer, and spring seasons, the growth of fir and spruce were initially highly correlated, followed by a downward trend (decreased correlation) and then, at the end of the season, another increase with increasing latitude (Figure 11a–c). However, during the autumn season, the correlation of fir started at $R^2 = 0.20$ at 30° latitude, followed by a downward trend up to 34° latitude, and then showed an upward trend up to 35° latitude. Conversely, spruce growth showed the opposite trend with increasing latitude (Figure 11d).

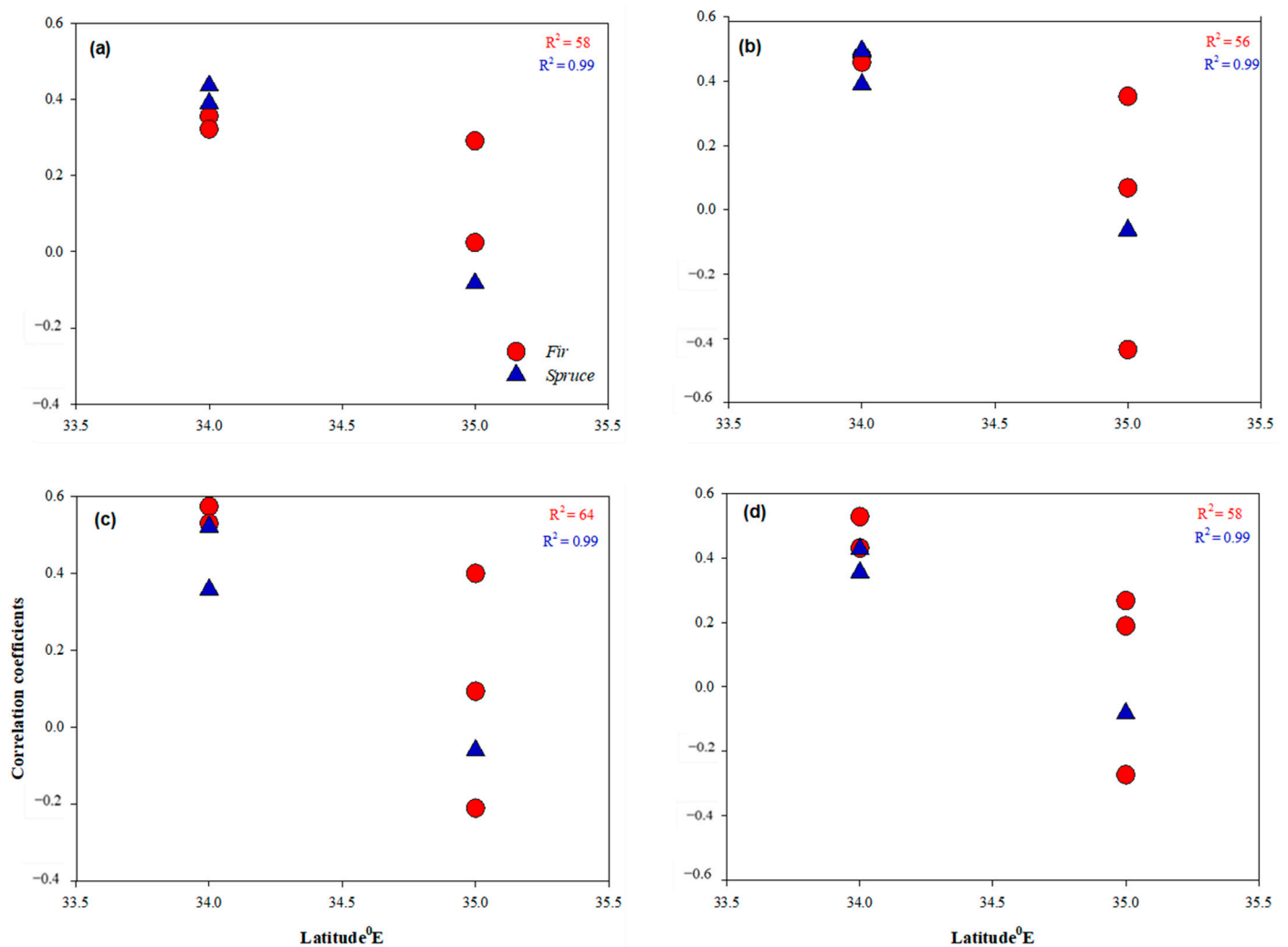


Figure 11. Variation of correlation coefficients between the tree-ring chronologies of spruce (blue triangles) and fir (red dots) and seasonal PDSI with latitudes from 1950 to 2018. (a) Winter (Dec–Feb), (b) spring (Mar–May), (c) summer (Jun–Jul), and (d) autumn (Sep–Nov).

4. Discussion

4.1. Tree-Ring Chronology Characteristics

The interseries correlation of $R^2 = 0.61$ using 306 years of tree-ring chronology in the Chaproat area of Northern Pakistan reported by Bandari et al. [37] is consistent with the results of our study with respect to fir. However, a slightly higher correlation was reported in Bandari et al. [37] for spruce ($R^2 = 0.68$) using 538 years of tree-ring chronology in the Shirial area of Northern Pakistan than in our study. In another study, Ahmed et al. [49] studied the dendroclimatology of fir and reported interseries correlations of 0.54 and 0.59 in the moist temperate forests of two localities in Northern Pakistan (Ayubia and Astore), respectively. The results reported by Ahmed et al. [49] are comparable to the interseries correlations (0.60 and 0.54 for NPKA and SHG, respectively) reported in our study. Similarly, Khan et al. [73] reported a correlation from 0.41 to 0.76 during a dendrochronological evaluation of fir in Kohistan (Northern Pakistan) based on 394 years, which is similar to the interseries correlation results for fir in this study (which gave a range of 0.48 to 0.60). Thapa et al. [82] studied the effect of changing climate on the tree-rings of fir in Himalayan Nepal and observed an intercorrelation of 0.42, similar to that found at the SHA sampling site in this study. Palmer et al. [83] studied dendrochronological research conducted in various areas of Pakistan and reported interseries correlations of 0.73 and 0.65 for spruce in the Chera and Naltar sites of Gilgit. These results are a little higher

than those in our study, which reported 0.49 and 0.55 for BSG and UDS, respectively. In contrast, Zafar et al. [50] reported a higher interseries correlation of 0.84 and 0.73 for spruce in the Haramosh and Bagrot sites of Gilgit Baltistan, Pakistan, respectively. Moreover, we observed clear climate variability in both species, with significant evidence for the occurrence of drought and humid years at specific intervals. The results of our research are comparable to those of Bhandari et al. [37], who reported suppression and accelerated growth for fir and spruce between the 17th and 20th centuries in Northern Pakistan. Similarly, Asad et al. [84] reported an acceleration in the radial growth of *Pinus wallichiana* in the northern areas since 1950. In another study by Thapa et al. [39], the radial growth of coniferous species in the adjacent mountain forests of Nepal was shown to have increased in the last few decades. Several other studies have also reported accelerated spruce radial growth from 1950 onwards in adjacent coniferous forests in India [85,86]. On the other hand, a period of suppression in the radial growth of fir in Kohistan and spruce in Haramosh valley of Northern Pakistan was observed in the 17th century [50,73].

4.2. Climate Growth Relationship of Fir and *Picea smithiana*

Our results show that the effect of climatic variables (temperature and precipitation) on the growth of fir and spruce varied for different study sites located at different topographic gradients. However, the influence of mean temperature on the growth of both species was more prominent than that of mean precipitation at the same sites. Spruce growth was negatively correlated with the mean annual temperature in May at SHG, similar to the findings of Ahmed et al. [69], who reported a negative correlation at Bagrot in Gilgit Baltistan (GB). Conversely, a negative correlation was observed in December and March in the Haramosh valley, GB [69]. Similarly, Ahmed et al. [67] reported a negative correlation for spruce growth in April and May in the Chera site, GB, and a positive correlation in June and July at the Naltar site, GB, which is consistent with our results (Figure 7a,c). The regional growth of fir was reported in the premonsoon period [87,88], and a negative correlation was reported for fir and spruce in premonsoon months [65]. Gaire et al. [89] found that the tree-ring width of *Abies* was significantly influenced by the temperature in June, July, and August compared to all other months.

Moreover, our study reported a positive correlation between spruce growth and temperature in June and August, similar to Wahab [90], who studied the spruce growth in the Dir district in Northern Pakistan and reported a correlation in June, July, and August. Altitude is a major topographic factor that influences the spatial distribution of forest species [74], and consequently affects the correlation of radial growth and climatic factors. For this reason, temperature is considered the most influential climatic factor compared with precipitation [91]. Therefore, the radial growth of fir and spruce is significantly correlated with temperature as a result of the high altitudes at the SHG and BSG sites [37,92].

Furthermore, our findings show that, generally, precipitation is positively correlated with the growth of fir in February, May, and September, whereas for spruce, there is a positive correlation in April, November, May, and June. However, a negative correlation was observed for both species in May (for *Picea smithiana*) and June. The results of this study are consistent with those of Bhandari et al. [37], who reported a positive correlation between precipitation and growth from March to July (for *Abies pindrow*) and in April (for *Picea smithiana*). Previous studies have also reported that moisture and precipitation positively impact the radial growth of conifer species not only in Northern Pakistan [68,69] but also in the surrounding region of the Himalayas [63]. Such dry conditions with high evapotranspiration may reduce the radial growth of coniferous species; however, warm winters and excellent summers increase the growth of fir and spruce [93–95]. Moreover, Yadav et al. [96] and Singh et al. [97] reported that the growth of coniferous species in Himalayan regions was sensitive to moisture availability and rainfall. Similarly, Sohar et al. [65] reported that rainfall before the monsoon positively influenced the radial growth of fir and spruce, whereas the impact of monsoon rainfall was less prominent. In our

research, *Abies* and *Picea* samples were collected from high elevation areas located in dry and semiarid ecological zones with low precipitation and moisture-deficient soil.

The PDSI was more strongly correlated with and influential in the growth of fir and spruce than precipitation and temperature (Figure 6b,c). This was also evident from the work of Bhandari et al. [37], who studied the same species in Northern Pakistan. The results of our study show that PDSI is strongly correlated with the growth of both species from May to October (Figure 6b). Ram [98] studied the relationship of fir growth and PDSI in India and found that PDSI is positively correlated with radial growth from June to September, congruent with our research findings (Figure 6b).

Similarly, Ram and Borgaonkar [88] reported the strong correlation of PDSI with the radial growth of fir and spruce from May to July. Furthermore, another study reported a strong correlation between tree growth (fir) and PDSI from March to October [88]. PDSI is strongly correlated with the growth of other coniferous species such as *Pinus wallichiana* in the spring season, as excess moisture is available [93]. Roibu et al. [99] also reported a significant correlation of PDSI with *Quercus* and *Fraxinus* from February to September. Additionally, Bhandari et al. [37] reported that PDSI is strongly and significantly correlated with the tree-ring width of fir and spruce throughout spring and summer (with the exception of August in the case of *Abies*), consistent with our findings. Van der Maaten-Theunissen et al. [92] reported that the growth of *Abies alba* and *Picea abies* is sensitive to summer PDSI and influenced by altitudinal gradient. Rai et al. [100] also reported such findings in the dendrochronology of *Abies spectabilis* along the altitudinal gradient.

4.3. Dendroclimatological Relationship with Latitude

Lyu et al. [101] reported relationships between the growth of coniferous trees and climatic factors at two different sites located at different latitudes (Finland and the Tibetan Plateau). The study reported that the correlation between summer temperature and radial growth changed from weaker (nonsignificant) at lower latitudes to a significant negative relationship at higher latitudes in the summer season. Furthermore, different growing seasons and moisture contents were reported at different latitudes [102,103], and a decrease in moisture availability and a higher evapotranspiration were reported at the lower latitudes of Tibetan Plateau compared to its upper latitude [104]. Lyu et al. [101] further reported that the growing season was experienced one month earlier at sites located at the northernmost latitude than at those situated at the southernmost latitudes. In another study, Jyske et al. [105] reported a one-month delay in the growing season at sites located at different latitudes; May was the starting month in southern latitudes, whereas in the southern latitudes of Finland, the initiation of the growing season was delayed to June. Mäkinen et al. [106] also studied the dendrochronology of *Picea abies* along the transect at different latitudes and altitudes in European forests. The temporal (decadal) radial growth of *Picea abies* and its correlation with climatic factors was studied, and variations in correlations were observed at various sampling sites located at different latitudes in Germany, Norway, and Finland. Bosela et al. [107] studied variations in the radial growth of *Picea abies* and climatic factors along a latitudinal gradient in European forests. The study reported a significant relationship (strong correlation) between the growth of *Picea abies* and climatic factors during the summer season, but this strong correlation was influenced by latitudinal differences and showed variations from lower to higher latitudes. Čater and Levanič [108] analyzed the growth of *Abies alba* and *Fagus sylvatica* and established its relationship with climatic factors and PDSI. The study reported variations in the radial growth of both species, yet the response of each species to the latitudinal gradient was different (the response of *Fagus* increased towards the southeast, whereas that of *Abies* decreased from northwest to southeast locations).

Many previous researchers have reported variations in the radial growth of *Abies alba* with respect to climatic factors along latitudinal gradients [109–112]. In their study, Liang et al. [113] stated that tree growth responses to changing climates cannot be fully quantified using climatic factors alone, and integration with other data is needed to explain

forest growth responses along the altitudinal gradient. Yasmeen et al. [114] studied the chronology of *Larix gmelinii* and *Pinus sylvestris* along the altitudinal gradient in northern China. The study reported an opposite behavior (trend) of correlation between the radial growth of both species and climatic factors (temperature and precipitation) from lower to higher latitudes.

5. Conclusions

In this study, we conducted a dendrochronological analysis of spruce and fir at five different sites in Northern Pakistan along the altitudinal gradient. The main objectives of the study were to investigate the significant climatic factors affecting the radial growth of spruce and fir pine at five ecological sites and to understand the relationship of latitudinal gradient and the growth–climate response of both species. A total of 219 samples (ring cores) were collected from both species at five different sites (SHG, UDS, BSG, NPKA, and SHA) in Northern Pakistan. The results for spruce and fir showed the occurrence of climate variability between 1950 and 2017.

In the case of spruce at SHG, the lowest tree-ring width was 0.54 in 1879, which was the most severe drought year, whereas the highest width was 1.42 in 1854, which was the most humid year. In UDS and BSG, the most severe drought years were 1892 and 1879, respectively, and the most humid years were 1822 and 1861, respectively. The highest climate variability was recorded in two periods, the first between 1804 and 1843, and the second between 1872 and 1900, whereas the lowest was found between 1915 and 1991. Similarly, in the case of fir, the highest climate variability was recorded in two periods, the first between 1819 and 1879, and the second between 1986 and 2017, whereas the lowest climate variability occurred during the first half of the 20th century. With respect to the relationship of growth with climatic factors, fir growth was found to be positively correlated with precipitation (in the summer season), mean temperature, and PDSI (in spring, summer, and autumn). The growth of spruce was similarly positively correlated with precipitation (in February, September, and May) and PDSI (in the summer and autumn seasons). However, no correlation with monthly temperature was observed.

Additionally, subsequent to the rapid warming of 1980, a considerable rise in the correlation coefficient was noted in the association of fir and spruce growth with seasonal precipitation and PDSI. This increased initially up to midlatitudes and then gradually decreased with increasing latitude (with the exception of some sites); thus, the correlation coefficient for radial growth of both species with seasonal temperature and PDSI demonstrated significant variation along the latitudinal gradient. Further in-depth research is necessary to assess the effects of a changing climate on important coniferous species in Northern Pakistan along the latitudinal gradient. The results of the current study are useful for climatic reconstruction.

Author Contributions: Conceptualization: X.W.; methodology, H.U. and A.K.; writing—original draft preparation, H.U., N.A. (Naveed Ahmad) and N.A. (Nizar Ali); writing—review and editing, Q.H., M.W.R. and I.H.; supervision, funding acquisition, X.W. All authors have read and agreed to the published version of the manuscript.

Funding: Funding was received from the Fund of Eco-Meteorological Innovation of the Open Laboratory in Northeast China, China Meteorological Bureau (atqx2018zd02).

Institutional Review Board Statement: Not applicable.

Informed Consent Statement: Not applicable.

Data Availability Statement: No supplementary data are available.

Conflicts of Interest: The authors declare no conflict of interest.

References

1. Jandl, R.; Spathelf, P.; Bolte, A.; Prescott, C.E. Forest adaptation to climate change—Is non-management an option? *Ann. For. Sci.* **2019**, *76*, 48. [\[CrossRef\]](#)
2. Stefanidis, S.; Alexandridis, V. Precipitation and potential evapotranspiration temporal variability and their relationship in two forest ecosystems in Greece. *Hydrology* **2021**, *8*, 160. [\[CrossRef\]](#)
3. Zindros, A.; Radoglou, K.; Milios, E.; Kitikidou, K. Tree line shift in the Olympus mountain (Greece) and climate change. *Forests* **2020**, *11*, 985. [\[CrossRef\]](#)
4. IPCC. Climate Change 2021: The physical science basis. In *Contribution of Working Group I to the Sixth Assessment Report of the Intergovernmental Panel on Climate Change*; Cambridge University Press: Cambridge, UK, 2021.
5. Pretzsch, H.; Biber, P.; Schütze, G.; Uhl, E.; Rötzer, T. Forest stand growth dynamics in Central Europe have accelerated since 1870. *Nat. Commun.* **2014**, *5*, 4967. [\[CrossRef\]](#) [\[PubMed\]](#)
6. Reed, C.C.; Ballantyne, A.P.; Cooper, L.A.; Sala, A. Limited evidence for CO₂-related growth enhancement in northern Rocky Mountain lodgepole pine populations across climate gradients. *Glob. Chang. Biol.* **2018**, *24*, 3922–3937. [\[CrossRef\]](#) [\[PubMed\]](#)
7. Rogers, B.M.; Jantz, P.; Goetz, S.J. Vulnerability of eastern US tree species to climate change. *Glob. Chang. Biol.* **2017**, *23*, 3302–3320. [\[CrossRef\]](#) [\[PubMed\]](#)
8. Kirschbaum, M.U. Will changes in soil organic carbon act as a positive or negative feedback on global warming? *Biogeochemistry* **2000**, *48*, 21–51. [\[CrossRef\]](#)
9. Boisvenue, C.; Running, S.W. Impacts of climate change on natural forest productivity—evidence since the middle of the 20th century. *Glob. Chang. Biol.* **2006**, *12*, 862–882. [\[CrossRef\]](#)
10. Bukhari, S.S.B.; Bajwa, G.A. *Development of National Response Strategy to Combat Impacts of Climate Change on Forest of Pakistan*; Pakistan Forest Institute Peshawar: Peshawar, Pakistan, 2012.
11. Camarero, J.J.; Fajardo, A. Poor acclimation to current drier climate of the long-lived tree species *Fitzroya cupressoides* in the temperate rainforest of southern Chile. *Agric. For. Meteorol.* **2017**, *239*, 141–150. [\[CrossRef\]](#)
12. Liu, B.; Liang, E.; Liu, K.; Camarero, J.J. Species- and elevation-dependent growth responses to climate warming of mountain forests in the Qinling Mountains, central China. *Forests* **2018**, *9*, 248. [\[CrossRef\]](#)
13. Davi, N.K.; D'Arrigo, R.; Jacoby, G.; Cook, E.; Anchukaitis, K.; Nachin, B.; Rao, M.; Leland, C. A long-term context (931–2005 CE) for rapid warming over Central Asia. *Quat. Sci. Rev.* **2015**, *121*, 89–97. [\[CrossRef\]](#)
14. Shi, C.; Masson-Delmotte, V.; Daux, V.; Li, Z.; Carré, M.; Moore, J.C. Unprecedented recent warming rate and temperature variability over the east Tibetan Plateau inferred from Alpine treeline dendrochronology. *Clim. Dyn.* **2015**, *45*, 1367–1380. [\[CrossRef\]](#)
15. Büntgen, U.; Myglan, V.S.; Ljungqvist, F.C.; McCormick, M.; Di Cosmo, N.; Sigl, M.; Kaplan, J.O. Cooling and societal change during the Late Antique Little Ice Age from 536 to around 660 AD. *Nat. Geosci.* **2016**, *9*, 231–236. [\[CrossRef\]](#)
16. Yang, Y.; Guan, J.; Yin, J.; Shao, B.; Li, H. Urinary levels of bisphenol analogues in residents living near a manufacturing plant in south China. *Chemosphere* **2014**, *112*, 481–486. [\[CrossRef\]](#)
17. Hadad, M.A.; González-Reyes, Á.; Roig, F.A.; Matsuksky, V.; Cherubini, P. Tree-ring-based hydroclimatic reconstruction for the northwest Argentine Patagonia since 1055 CE and its teleconnection to large-scale atmospheric circulation. *Glob. Planet. Chang.* **2021**, *202*, 103496. [\[CrossRef\]](#)
18. Allen, K.J.; Freund, M.B.; Palmer, J.G.; Simkin, R.; Williams, L.; Brookhouse, M.; Cook, E.R.; Stewart, S.; Baker, P.J. Hydroclimate extremes in a north Australian drought reconstruction asymmetrically linked with Central Pacific Sea surface temperatures. *Glob. Planet. Chang.* **2020**, *195*, 103329. [\[CrossRef\]](#)
19. Panthi, S.; Fan, Z.X.; van der Sleen, P.; Zuidema, P.A. Long-term physiological and growth responses of Himalayan fir to environmental change are mediated by mean climate. *Glob. Chang. Biol.* **2020**, *26*, 1778–1794. [\[CrossRef\]](#)
20. Salick, J.; Ghimire, S.K.; Fang, Z.; Dema, S.; Konchar, K.M. Himalayan alpine vegetation, climate change and mitigation. *J. Ethnobiol.* **2014**, *34*, 276–293. [\[CrossRef\]](#)
21. Schwab, N.; Kaczka, R.J.; Janecka, K.; Böhner, J.; Chaudhary, R.P.; Scholten, T.; Schickhoff, U. Climate change-induced shift of tree growth sensitivity at a central Himalayan treeline ecotone. *Forests* **2018**, *9*, 267. [\[CrossRef\]](#)
22. Salzer, M.W.; Hughes, M.K.; Bunn, A.G.; Kipfmüller, K.F. Recent unprecedented tree-ring growth in bristlecone pine at the highest elevations and possible causes. *Proc. Natl. Acad. Sci. USA* **2009**, *106*, 20348–20353. [\[CrossRef\]](#)
23. Qi, Z.; Liu, H.; Wu, X.; Hao, Q. Climate-driven speedup of alpine treeline forest growth in the Tianshan Mountains, northwestern China. *Glob. Chang. Biol.* **2015**, *21*, 816–826. [\[CrossRef\]](#) [\[PubMed\]](#)
24. Liang, E.; Shao, X.; Xu, Y. Tree-ring evidence of recent abnormal warming on the southeast Tibetan Plateau. *Theor. Appl. Climatol.* **2009**, *98*, 9–18. [\[CrossRef\]](#)
25. Bayramzadeh, V.; Zhu, H.; Lu, X.; Attarod, P.; Zhang, H.; Li, X.; Asad, F.; Liang, E. Temperature variability in northern Iran during the past 700 years. *Sci. Bull.* **2018**, *63*, 462–464. [\[CrossRef\]](#)
26. Hartl-Meier, C.; Dittmar, C.; Zang, C.; Rothe, A. Mountain forest growth response to climate change in the Northern Limestone Alps. *Trees* **2014**, *28*, 819–829. [\[CrossRef\]](#)
27. Zhang, X.; Liu, X.; Zhang, Q.; Zeng, X.; Xu, G.; Wu, G.; Wang, W. Species-specific tree growth and intrinsic water-use efficiency of Dahurian larch (*Larix gmelinii*) and Mongolian pine (*Pinus sylvestris* var. *Mongolica*) growing in a boreal permafrost region of the greater Hinggan Mountains, northeastern China. *Agric. For. Meteorol.* **2018**, *248*, 145–155. [\[CrossRef\]](#)

28. Liang, E.; Dawadi, B.; Pederson, N.; Eckstein, D. Is the growth of birch at the upper timberline in the Himalayas limited by moisture or by temperature? *Ecology* **2014**, *95*, 2453–2465. [[CrossRef](#)]
29. Liang, E.; Leuschner, C.; Dulamsuren, C.; Wagner, B.; Hauck, M. Global warming related tree growth decline and mortality on the north-eastern Tibetan plateau. *Clim. Chang.* **2016**, *134*, 163–176. [[CrossRef](#)]
30. Weigel, R.; Muffler, L.; Klisz, M.; Kreyling, J.; van der Maaten-Theunissen, M.; Wilmking, M.; van der Maaten, E. Winter matters: Sensitivity to winter climate and cold events increases towards the cold distribution margin of European beech (*Fagus sylvatica* L.). *J. Biogeogr.* **2018**, *45*, 2779–2790. [[CrossRef](#)]
31. Harvey, J.E.; Smiljanić, M.; Scharnweber, T.; Buras, A.; Cedro, A.; Cruz-García, R.; Drobyshev, I.; Janecka, K.; Jansons, Ā.; Kaczka, R.; et al. Tree growth influenced by warming winter climate and summer moisture availability in northern temperate forests. *Glob. Chang. Biol.* **2020**, *26*, 2505–2518. [[CrossRef](#)]
32. Zeng, X.; Evans, M.N.; Liu, X.; Wang, W.; Xu, G.; Wu, G.; Zhang, L. Spatial patterns of precipitation-induced moisture availability and their effects on the divergence of conifer stem growth in the western and eastern parts of China's semi-arid region. *For. Ecol. Manag.* **2019**, *451*, 117524. [[CrossRef](#)]
33. Stajić, B.; Kazimirović, M.; Dukić, V.; Radaković, N. First Dendro-climatological Insight into Austrian Pine (*Pinus nigra* Arnold) Climate-Growth Relationship in Belgrade Area, Serbia. *South-East Eur.* **2020**, *11*, 127–134. [[CrossRef](#)]
34. Manrique-Alba, À.; Beguería, S.; Molina, A.J.; González-Sanchis, M.; Tomàs-Burguera, M.; Del Campo, A.D.; Camarero, J.J. Long-term thinning effects on tree growth, drought response and water use efficiency at two Aleppo pine plantations in Spain. *Sci. Total Environ.* **2020**, *728*, 138536. [[CrossRef](#)] [[PubMed](#)]
35. Zhang, Y.; Cao, R.; Yin, J.; Tian, K.; Xiao, D.; Zhang, W.; Yin, D. Radial growth response of major conifers to climate change on Haba Snow Mountain, Southwestern China. *Dendrochronologia* **2020**, *60*, 125682. [[CrossRef](#)]
36. Iqbal, J.; Ahmed, M.; Siddiqui, M.F.; Khan, A. Tree ring studies from some conifers and present condition of forest of Shangla district of Khyber Pukhtunkhwa Pakistan. *Pak. J. Bot.* **2020**, *52*, 653–662. [[CrossRef](#)]
37. Bhandari, S.; Speer, J.H.; Khan, A.; Ahmed, M. Drought signal in the tree rings of three conifer species from Northern Pakistan. *Dendrochronologia* **2020**, *63*, 125742. [[CrossRef](#)]
38. Thapa, U.K.; George, S.S.; Kharal, D.K.; Gaire, N.P. Tree growth across the Nepal Himalaya during the last four centuries. *Prog. Phys. Geogr.* **2017**, *41*, 478–495. [[CrossRef](#)]
39. Spach. *Histoire Naturelle des Vegetaux*; V. 11; Labrairie Encyclopedique de Roret: Paris, France, 1841. Available online: <https://www.biodiversitylibrary.org/page/31487119#page/434/mode/1up> (accessed on 9 March 2019).
40. Shrestha, K.B.; Hofgaard, A.; Vandvik, V. Tree-growth response to climatic variability in two climatically contrasting treeline ecotone areas, central Himalaya, Nepal. *Can. J. For. Res.* **2015**, *45*, 1643–1653. [[CrossRef](#)]
41. Rayback, S.A.; Shrestha, K.B.; Hofgaard, A. Growth variable-specific moisture and temperature limitations in co-occurring alpine tree and shrub species, central Himalayas, Nepal. *Dendrochronologia* **2017**, *44*, 193–202. [[CrossRef](#)]
42. Zhuang, L.; Axmacher, J.C.; Sang, W. Different radial growth responses to climate warming by two dominant tree species at their upper altitudinal limit on Changbai Mountain. *J. For. Res.* **2017**, *28*, 795–804. [[CrossRef](#)]
43. Keenan, R.J.; Reams, G.A.; Achard, F.; de Freitas, J.V.; Grainger, A.; Lindquist, E. Dynamics of global forest area: Results from the FAO Global Forest Resources Assessment. *For. Ecol. Manag.* **2015**, *352*, 9–20. [[CrossRef](#)]
44. Xu, H.J.; Wang, X.P.; Zhang, X.X. Decreased vegetation growth in response to summer drought in Central Asia from 2000 to 2012. *Int. J. Appl. Earth Obs. Geoinf.* **2016**, *52*, 390–402. [[CrossRef](#)]
45. Sun, J.; Liu, Y. Age-independent climate-growth response of Chinese pine (*Pinus tabulaeformis* Carrière) in North China. *Trees* **2015**, *29*, 397–406. [[CrossRef](#)]
46. Khan, N.; Ahmed, M.; Wahab, M. Dendroclimatic potential of *Picea smithiana* (Wall) Boiss, from Afghanistan. *Pak. J. Bot.* **2008**, *40*, 1063–1070.
47. Laxton, S.C.; Smith, D.J. Dendrochronological reconstruction of snow avalanche activity in the Lahul Himalaya, Northern India. *Nat. Hazards* **2009**, *49*, 459–467. [[CrossRef](#)]
48. Ahmed, M.; Wahab, M.; Khan, N.; Siddiqui, M.F.; Khan, M.U.; Hussain, S.T. Age and growth rates of some gymnosperms of Pakistan: A dendrochronological approach. *Pak. J. Bot.* **2009**, *41*, 849–860.
49. Ahmed, M.; Wahab, M.; Khan, N.A.S.R.U.L.L.A.H.; Zafar, M.U.; Palmer, J. Tree-ring chronologies from upper indus basin of karakorum range, Pakistan. *Pak. J. Bot.* **2010**, *42*, 295–308.
50. Zafar, M.U.; Ahmed, M.; Farooq, M.A.; Akbar, M.; Hussain, A. Standardized tree ring chronologies of *Picea smithiana* from two new sites of Northern area Pakistan. *World Appl. Sci. J.* **2010**, *11*, 1531–1536.
51. Thapa, U.K.; Shah, S.K.; Gaire, N.P.; Bhujju, D.R. Spring temperatures in the far-western Nepal Himalaya since AD 1640 reconstructed from *Picea smithiana* tree-ring widths. *Clim. Dyn.* **2015**, *45*, 2069–2081. [[CrossRef](#)]
52. Seim, A.; Omurova, G.; Azisov, E.; Musuraliev, K.; Aliev, K.; Tulyaganov, T.; Nikolyai, L.; Botman, E.; Helle, G.; Dorado Liñan, I.; et al. Climate Change Increases Drought Stress of Juniper Trees in the Mountains of Central Asia. *PLoS ONE* **2016**, *11*, e0153888. [[CrossRef](#)]
53. Solomina, A.; Maximova, A.; Cook, A. *Picea Schrenkian* ring width and density at the upper and lower tree limits in the Tien Shan Mountains (Kirgizstan Republic) as a source of paleoclimatic information. *Geogr. Environ. Sustain.* **2014**, *7*, 66–79. [[CrossRef](#)]

54. Zhang, T.; Yuan, Y.; He, Q.; Wei, W.; Diushen, M.; Shang, H.; Zhang, R. Development of tree-ring width chronologies and tree-growth response to climate in the mountains surrounding the Issyk-Kul Lake, Central Asia. *Dendrochronologia* **2014**, *32*, 230–236. [[CrossRef](#)]
55. Lyu, L.; Deng, X.; Zhang, Q.B. Elevation pattern in growth coherency on the southeastern Tibetan Plateau. *PLoS ONE* **2016**, *11*, e0163201. [[CrossRef](#)]
56. Rauning, A. Combined view of various tree ring parameters from different habitats in Tibet for the reconstruction of seasonal aspects of Asian Monsoon variability. *Palaeobotanist* **2001**, *50*, 1–12.
57. Fan, Z.; Bräuning, A.; Cao, K. Tree-ring based drought reconstruction in the central Hengduan Mountains region (China) since AD 1655. *Int. J. Climatol.* **2008**, *28*, 1879–1887. [[CrossRef](#)]
58. Korner, C. *Alpine Treelines*; Springer: Basel, Switzerland, 2012.
59. Fan, Z.X.; Bräuning, A.; Cao, K.F.; Zhu, S.D. Growth–climate responses of high elevation conifers in the central Hengduan Mountains, southwestern China. *For. Ecol. Manag.* **2009**, *258*, 306–313. [[CrossRef](#)]
60. Latreille, A.; Davi, H.; Huard, F.; Pichot, C. Variability of the climate-radial growth relationship among *Abies alba* trees and populations along altitudinal gradients. *For. Ecol. Manag.* **2017**, *396*, 150–159. [[CrossRef](#)]
61. Wang, W.; Jia, M.; Wang, G.; Zhu, W.; McDowell, N.G. Rapid warming forces contrasting growth trends of subalpine fir (*Abies fabri*) at higher- and lower-elevations in the eastern Tibetan Plateau. *For. Ecol. Manag.* **2017**, *402*, 135–144. [[CrossRef](#)]
62. Kharal, D.K.; Thapa, U.K.; St. George, S.; Meilby, H.; Rayamajhi, S.; Bhujju, D.R. Tree-climate relations along an elevational transect in Manang Valley, central Nepal. *Dendrochronologia* **2017**, *41*, 57–64. [[CrossRef](#)]
63. Panthi, S.; Bräuning, A.; Zhou, Z.K.; Fan, Z.X. Tree rings reveal recent intensified spring drought in the central Himalaya, Nepal. *Glob. Planet. Chang.* **2017**, *157*, 26–34. [[CrossRef](#)]
64. Sohar, K.; Altman, J.; Lehečková, E.; Doležal, J. Growth–climate relationships of Himalayan conifers along elevational and latitudinal gradients. *Int. J. Climatol.* **2017**, *37*, 2593–2605. [[CrossRef](#)]
65. Li, J.; Shi, J.; Zhang, D.D.; Yang, B.; Fang, K.; Yue, P.H. Moisture increase in response to high-altitude warming evidenced by tree-rings on the southeastern Tibetan Plateau. *Clim. Dyn.* **2017**, *48*, 649–660. [[CrossRef](#)]
66. Lloyd, A.H.; Bunn, A.G.; Berner, L. A latitudinal gradient in tree growth response to climate warming in the Siberian taiga. *Glob. Chang. Biol.* **2011**, *17*, 1935–1945. [[CrossRef](#)]
67. Ahmed, M.; Palmer, J.; Khan, N.; Wahab, M.; Fenwick, P.; Esper, J.; Cook, E. The dendroclimatic potential of conifers from northern Pakistan. *Dendrochronologia* **2011**, *29*, 77–88. [[CrossRef](#)]
68. Ahmed, M.; Khan, N.; Wahab, M.; Zafar, U.; Palmer, J. Climate/growth correlations of tree species in the Indus basin of the Karakorum range, north Pakistan. *IAWA J.* **2012**, *33*, 51–61. [[CrossRef](#)]
69. Ahmed, M.; Zafar, M.U.; Hussain, A.; Akbar, M.; Wahab, M.; Khan, N. Dendroclimatic and dendrohydrological response of two tree species from Gilgit valleys. *Pak. J. Bot.* **2013**, *45*, 987–992.
70. Ahmed, M.; Zafar, M.U. The Status of Tree-Ring Analysis in Pakistan. *FUUAST J. Biol.* **2014**, *4*, 13–19.
71. Zafar, M.U.; Ahmed, M.; Rao, M.P.; Buckley, B.M.; Khan, N.; Wahab, M.; Palmer, J. Karakorum temperature out of phase with hemispheric trends for the past five centuries. *Clim. Dyn.* **2015**, *46*, 1943–1952. [[CrossRef](#)]
72. Iqbal, J.; Ahmed, M.; Siddiqui, M.F.; Khan, A.; Wahab, M. Age and radial growth analysis of conifer tree species from Shangla, Pakistan. *Pak. J. Bot.* **2017**, *49*, 69–72.
73. Khan, A.; Ahmed, M.; Siddiqui, M.F.; Iqbal, J.; Gaire, N.P. Dendrochronological potential of *Abies pindrow* Royle from Indus Kohistan, Khyber Pakhtunkhwa (KPK) Pakistan. *Pak. J. Bot.* **2018**, *50*, 365–369.
74. Ahmad, N.; Ashraf, M.I.; Malik, S.U.; Qadir, I.; Malik, N.A.; Khan, K. Impact of Climatic and Topographic Factors on Distribution of Sub-tropical and Moist Temperate Forests in Pakistan. *Geomorphol. Relief Process. Environ.* **2020**, *26*, 157–172. [[CrossRef](#)]
75. Ali, A.; Ashraf, M.I.; Gulzar, S.; Akmal, M. Estimation of forest carbon stocks in temperate and subtropical mountain systems of Pakistan: Implications for REDD+ and climate change mitigation. *Environ. Monit. Assess.* **2020**, *192*, 198. [[CrossRef](#)] [[PubMed](#)]
76. Holmes, R.L. Computer-assisted quality control in tree-ring dating and measurement. *Tree-Ring Bull.* **1983**, *43*, 69–78.
77. Duan, J.; Wu, P.; Ma, Z.; Duan, Y. Unprecedented recent late-summer warm extremes recorded in tree-ring density on the Tibetan Plateau. *Environ. Res. Lett.* **2020**, *15*, 024006. [[CrossRef](#)]
78. Dai, A.; Trenberth, K.E.; Qian, T. A global dataset of Palmer Drought Severity Index for 1870–2002: Relationship with soil moisture and effects of surface warming. *J. Hydrometeorol.* **2004**, *5*, 1117–1130. [[CrossRef](#)]
79. Rocha, E.; Gunnarson, B.E.; Holzkämper, S. Reconstructing summer precipitation with mxr data from *Pinus sylvestris* growing in the Stockholm archipelago. *Atmosphere* **2020**, *11*, 790. [[CrossRef](#)]
80. Khaleghi, M.R. Application of dendroclimatology in evaluation of climatic changes. *J. For. Sci.* **2018**, *64*, 139–147. [[CrossRef](#)]
81. Shah, H.; Jehan, N.; Rehman, S.S.; Bukhari, S.S.B. Comparative Study of Climate Change and its Impact on Ring-Widths of Spruce (*Picea smithiana*) at Kalam and Kaghan Forest Divisions, Khyber Pakhtunkhwa, Pakistan. *Sarhad J. Agric.* **2019**, *35*, 788–797. [[CrossRef](#)]
82. Thapa, U.K.; Shah, S.K.; Gaire, N.P. Influence of climate on radial growth of *Abies pindrow* in western Nepal Himalaya. *Banko Janakari* **2013**, *23*, 14–19. [[CrossRef](#)]
83. Palmer, J.; Ahmed, M.; Khan, Z. Application of tree-ring research in Pakistan. *FUUAST J. Biol.* **2011**, *1*, 19–25.
84. Asad, F.; Zhu, H.; Zhang, H.; Liang, E.; Muhammad, S.; Farhan, S.B.; Hussain, I.; Wazir, M.A.; Ahmed, M.; Esper, J. Are Karakoram temperatures out of phase compared to hemispheric trends? *Clim. Dyn.* **2016**, *48*, 3381–3390. [[CrossRef](#)]

85. Borgaonkar, H.P.; Sikder, A.B.; Ram, S. High altitude forest sensitivity to the recent warming: A tree-ring analysis of conifers from Western Himalaya, India. *Quat. Int.* **2011**, *236*, 158–166. [[CrossRef](#)]
86. Shah, S.K.; Pandey, U.; Mehrotra, N. Precipitation reconstruction for the Lidder Valley, Kashmir Himalaya using tree-rings of *Cedrus deodara*. *Int. J. Climatol.* **2018**, *38*, 758–773. [[CrossRef](#)]
87. Borgaonkar, H.P.; Pant, G.B.; Kumar, K.R. Tree-ring chronologies from western Himalaya and their dendroclimatic potential. *IAWA J.* **1999**, *20*, 295–309. [[CrossRef](#)]
88. Ram, S.; Borgaonkar, H.P. Growth response of conifer trees from high-altitude region of western Himalaya. *Curr. Sci.* **2013**, *105*, 225–231.
89. Gaire, N.P.; Fan, Z.X.; Bräuning, A.; Panthi, S.; Rana, P.; Shrestha, A.; Bhujju, D.R. *Abies spectabilis* shows stable growth relations to temperature, but changing response to moisture conditions along an elevation gradient in the central Himalaya. *Dendrochronologia* **2020**, *60*, 125675. [[CrossRef](#)]
90. Wahab, M. Population Dynamics and Dendrochronological Potential of Pine Tree Species from District Dir. Ph.D. Thesis, Federal Urdu University of Arts, Science and Technology, Karachi, Pakistan, 2011.
91. Häusser, M.; Szymczak, S.; Garel, E.; Santoni, S.; Huneau, F.; Bräuning, A. Growth variability of two native pine species on Corsica as a function of elevation. *Dendrochronologia* **2019**, *54*, 49–55. [[CrossRef](#)]
92. van der Maaten-Theunissen, M.; Kahle, H.P.; van der Maaten, E. Drought sensitivity of Norway spruce is higher than that of silver fir along an altitudinal gradient in southwestern Germany. *Ann. For. Sci.* **2013**, *70*, 185–193. [[CrossRef](#)]
93. Sigdel, S.R.; Wang, Y.; Camarero, J.J.; Zhu, H.; Liang, E.; Peñuelas, J. Moisture-mediated responsiveness of treeline shifts to global warming in the Himalayas. *Glob. Chang. Biol.* **2018**, *24*, 5549–5559. [[CrossRef](#)]
94. Liang, E.; Camarero, J.J. Threshold-dependent and non-linear associations between temperature and tree growth at and below the alpine treeline. *Trees* **2018**, *32*, 661–662. [[CrossRef](#)]
95. Gaire, N.P.; Dhakal, Y.R.; Shah, S.K.; Fan, Z.X.; Bräuning, A.; Thapa, U.K.; Bhujju, D.R. Drought (scPDSI) reconstruction of trans-Himalayan region of central Himalaya using *Pinus wallichiana* tree-rings. *Palaeogeogr. Palaeoclimatol. Palaeoecol.* **2019**, *514*, 251–264. [[CrossRef](#)]
96. Yadav, R.R.; Mishra, K.G.; Kotila, B.; Upreti, N. Premonsoon precipitation variability in Kumaon Himalaya, India over a perspective of ~300 years. *Quat. Int.* **2014**, *325*, 213–219. [[CrossRef](#)]
97. Singh, S.P.; Singh, R.D.; Gumber, S.U.R.A.B.H.I.; Bhatt, S.P.A.R.S.H. Two principal precipitation regimes in Himalayas and their influence on tree distribution. *Trop. Ecol.* **2017**, *58*, 679–691.
98. Ram, S. Tree growth–climate relationships of conifer trees and reconstruction of summer season Palmer Drought Severity Index (PDSI) at Pahalgam in Srinagar, India. *Quat. Int.* **2012**, *254*, 152–158. [[CrossRef](#)]
99. Roibu, C.C.; Sfeclă, V.; Mursa, A.; Ionita, M.; Nagavciuc, V.; Chiriloaei, F.; Popa, I. The Climatic Response of Tree Ring Width Components of Ash (*Fraxinus excelsior* L.) and Common Oak (*Quercus robur* L.) from Eastern Europe. *Forests* **2020**, *11*, 600. [[CrossRef](#)]
100. Rai, S.; Dawadi, B.; Wang, Y.; Lu, X.; Ru, H.; Sigdel, S.R. Growth response of *Abies spectabilis* to climate along an elevation gradient of the Manang valley in the central Himalayas. *J. For. Res.* **2019**, *31*, 2245–2254. [[CrossRef](#)]
101. Lyu, L.; Zhang, Q.B.; Pellatt, M.G.; Büntgen, U.; Li, M.H.; Cherubini, P. Drought limitation on tree growth at the Northern Hemisphere’s highest tree line. *Dendrochronologia* **2019**, *53*, 40–44. [[CrossRef](#)]
102. Rossi, S.; Deslauriers, A.; Anfodillo, T.; Carraro, V. Evidence of threshold temperatures for xylogenesis in conifers at high altitudes. *Oecologia* **2007**, *152*, 1–12. [[CrossRef](#)]
103. Henttonen, H.M.; Mäkinen, H.; Nöjd, P. Seasonal dynamics of the radial increment of Scots pine and Norway spruce in the southern and middle boreal zones in Finland. *Can. J. For. Res.* **2009**, *39*, 606–618. [[CrossRef](#)]
104. Lv, L.X.; Zhang, Q.B. Asynchronous recruitment history of *Abies spectabilis* along an altitudinal gradient in the Mt. Everest region. *J. Plant Ecol.* **2012**, *5*, 147–156. [[CrossRef](#)]
105. Jyske, T.; Mäkinen, H.; Kalliokoski, T.; Nöjd, P. Intra-annual tracheid production of Norway spruce and Scots pine across a latitudinal gradient in Finland. *Agric. For. Meteorol.* **2014**, *194*, 241–254. [[CrossRef](#)]
106. Mäkinen, H.; Nöjd, P.; Kahle, H.P.; Neumann, U.; Tveite, B.; Mielikäinen, K.; Spiecker, H. Radial growth variation of Norway spruce (*Picea abies* (L.) Karst.) across latitudinal and altitudinal gradients in central and northern Europe. *For. Ecol. Manag.* **2002**, *171*, 243–259. [[CrossRef](#)]
107. Bosela, M.; Tumajer, J.; Cienciala, E.; Dobor, L.; Kulla, L.; Marčič, P.; Šebeň, V. Climate warming induced synchronous growth decline in Norway spruce populations across biogeographical gradients since 2000. *Sci. Total Environ.* **2020**, *752*, 141794. [[CrossRef](#)] [[PubMed](#)]
108. Čater, M.; Levanič, T. Beech and silver fir’s response along the Balkan’s latitudinal gradient. *Sci. Rep.* **2019**, *9*, 16269. [[CrossRef](#)] [[PubMed](#)]
109. Gazol, A.; Ibáñez, R. Plant species composition in a temperate forest: Multi-scale patterns and determinants. *Acta Oecol.* **2010**, *36*, 634–644. [[CrossRef](#)]
110. Diaci, J.; Rozenberger, D.; Anic, I.; Mikac, S.; Saniga, M.; Kucbel, S.; Ballian, D. Structural dynamics and synchronous silver fir decline in mixed old-growth mountain forests in Eastern and Southeastern Europe. *Forestry* **2011**, *84*, 479–491. [[CrossRef](#)]
111. Ficko, A.; Poljanec, A.; Boncina, A. Do changes in spatial distribution, structure and abundance of silver fir (*Abies alba* Mill.) indicate its decline? *For. Ecol. Manag.* **2011**, *261*, 844–854. [[CrossRef](#)]

112. Castagneri, D.; Nola, P.; Motta, R.; Carrer, M. Summer climate variability over the last 250 years differently affected tree species radial growth in a mesic *Fagus–Abies–Picea* old-growth forest. *For. Ecol. Manag.* **2014**, *320*, 21–29. [[CrossRef](#)]
113. Liang, P.; Wang, X.; Sun, H.; Fan, Y.; Wu, Y.; Lin, X.; Chang, J. Forest type and height are important in shaping the altitudinal change of radial growth response to climate change. *Sci. Rep.* **2019**, *9*, 1336. [[CrossRef](#)]
114. Yasmeen, S.; Wang, X.; Zhao, H.; Zhu, L.; Yuan, D.; Li, Z.; Han, S. Contrasting climate-growth relationship between *Larix gmelinii* and *Pinus sylvestris* var. *mongolica* along a latitudinal gradient in Daxing'an Mountains, China. *Dendrochronologia* **2019**, *58*, 125645. [[CrossRef](#)]